Electronic Supplementary Material (ESI) for CrystEngComm.


Supporting information for

# Enantioselective Enrichment of Chiral 1-Phenylethanol in the Camphor-Based Chiral Metal-Organic Framework CFA-22

Richard Röß-Ohlenroth, [a‡] Katharina Knippen, [a‡] Maryana Kraft, [a] and Dirk Volkmer [a*]

Corresponding author: Prof. Dr. Dirk Volkmer
E-mail: dirk.volkmer(at)physik.uni-augsburg.de
Tel.: +49 (0) 821/598-3032
Fax: +49 (0) 821/598-5955

# Table of Contents

# 1. Experimental section

**Materials and general methods**

(R)-(+)-1-Phenylethanol (99%, ee 97+%, Alfa Aesar), (S)-(-)-1-phenylethanol (>98.0%, TCI), (±)-1-phenylethanol (>98%, TCI), n-heptane (HPLC grade, >99%, Alfa Aesar), 2-propanol (≥99,8%, HiPerSolv CHROMANORM® für die HPLC, VWR), methanol (≥99,8%, VWR), (S)-(-)-camphor (>98.0%, TCI), (R)-(+)-camphor (98%, Alfa Aesar), THF (99.85%, extra dry, unstabilized, AcroSeal™, Acros), nBuLi (1.6 M in hexane, Aldrich), diisopropylamine (99.5%, Aldrich), hydrazine monohydrochloride (Riedel-de Haën), hydrazine monohydrate (80% in water, >98%, Merck), and 1,3,5-benzenetricarboxylic acid chloride (98%, Thermo Scientific Chemicals) were used as obtained from the commercial supplier.

Melting points were measured with a Krüss KSP1N melting point meter. Fourier transform infrared (FTIR) spectra were recorded with ATR in the range 4000–400 $cm^{-1}$ with a measurement period of 32 scans on a Bruker Equinox 55 IR spectrometer. NMR spectra were recorded on a Mercury plus 400 high-resolution system (Fa. Varian Deutschland GmbH). $^{1}H$ NMR (400 MHz) and $^{13}C$ NMR (100 MHz) chemical shifts are given in ppm relative to the solvent signal. Molecular masses were measured with a Q-Tof Ultima mass spectrometer (Micromass) equipped with an ESI source. Mass spectra were calibrated using phosphoric acid. The composition of the ions was verified by a comparison between experimental and theoretical mass values. Thermogravimetric analysis (TGA) was performed with a TGA Q500 analyzer in the temperature range of 25–700 °C under a nitrogen flow at a heating rate of 5 K $min^{-1}$. SEM images and energy-dispersive X-ray spectroscopy (EDX) were performed with a Zeiss cross beam 550. The optical rotations were measured in chloroform using a Jasco P-2000 polarimeter using standard conditions (25.00 °C, 589 nm), with the rotational value as the average of at least 15 consecutive measurements. The powder X-ray diffraction (PXRD) data were collected with a Seifert PXRD 3003 TT- powder diffractometer with a Meteor 1D detector operating at room temperature using Copper K$\alpha$1Radiation ($\lambda$= 1.54187) if not stated otherwise. The measured range of 2$\theta$ was from 4 to 50°. VTPXRD determinations were performed with a PANalytical (Empyran) diffractometer, collecting X-ray diffraction data in the 2θ range from 5 to 40 ° with a step width of 0.013. The diffractometer was equipped with a Bragg-Brentano$^{HD}$ mirror and a reactor chamber from Anton Paar (CHC plus reactor, z-axis and air cooling). The X-ray tube was operated with 40 kV and 40 mA and a nickel filter was used to suppress $K_\beta$ radiation. The collection was carried out by means of a PIXcel$^{3D}$ 2x2 detector and a counting time of 294 s (Cu-$K_\alpha$ radiation, Bragg–Brentano geometry).

**Linker syntheses**

The described syntheses were carried out with R-camphor but can be conducted analogous with S-camphor.

(1R,1'R,1''R,4R,4'R,4''R)-3,3',3''-(benzene-1,3,5-tricarbonyl)tris(1,7,7-trimethylbicyclo[2.2.1]heptan-2-one) (**R-1**): Lithiumdiisopropylamide (LDA) was produced in situ by the reaction of diisopropylamine (4.4 mL, 10 mmol) and n-butyllithium (1.6 M in hexane, 18.75 mL, 10 mmol) under Schlenk conditions in dry THF (50 mL) at -20°C. To the LDA solution, (R/S)-camphor (4.75 g, 30 mmol) in 30 mL of dry THF was added and stirred for 30 min. Then, 1,3,5-benzenetricarboxylic acid chloride (1.8 g, 10 mmol) in 20 mL of dry THF was added slowly and stirred at -20°C for two hours. Then the solution was led to room temperature and stirred for additional 20 hours. The orange solution was then poured into 100 mL of water, washed with diluted HCl until neutral pH and extracted with diethyl ether. After washing with brine and drying with $NaSO_4$, a yellow oil was obtained. The NMR shows an intensive keto-enol tautomeric behaviour. However, the successful threefold substitution could be confirmed by mass spectrometry; MS (HR-ESI$^-$): m/z 611.3382, $[C_{39}H_{48}O_6 - H^-]^-$ requires 611.3378. The crude product (5.56 g, yield: 90%) was used without further purification directly in synthesis of the **4S,7R-H$_3$tristmi** ligand.

1,3,5-tris((4S,7R)-7,8,8-trimethyl-4,5,6,7-tetrahydro-1H-4,7-methanoindazol-3-yl)benzene **(4S,7R-H$_3$tristmi):** Compound **R-1** (5.56 g, 9 mmol) in 130 mL of methanol, hydrazine monohydrochloride (3.08 g, 45 mmol) and hydrazine monohydrate (15 mL, 80% in water, 24.7 mmol) were stirred under reflux for three days. The formed colourless precipitate was isolated via filtration, washed with cold methanol, and dried to obtain 3.55 g of the product (yield: 98%). M.p.> 360 °C; $^{1}H$ NMR: (400 MHz, $CDCl_3$:MeOD = 5:1, 20°C) δ 7.63 (s, 3H), 2.95 (d, J=3.6 Hz, 3H), 2.06 (m, 3H), 1.78 (m, 3H), 1.20 (s, 6H), 1.17 (s, 9H), 0.86 (s, 9H), 0.59 (s, 9H) ppm; $^{13}C$ (400 MHz, $CDCl_3$:MeOD = 1:5, 20°C) δ 170.44, 138.94, 135.96, 128.49, 125.62, 65.30, 54.31, 52.62, 37.42, 30.75, 24.24, 23.23, 22.92, 14.01 ppm; MS (HR-ESI$^-$): m/z 599.3837, $[C_{39}H_{48}N_6 - H^-]^-$ requires 599.3868; specific rotation: 147.29°ml/gdm. IR (ν($cm^{-1}$)): 3290 (m), 3259 (s), 3192 (w), 3128 (w), 3056 (w), 2981 (m), 2913 (w), 2594 (w), 1619(s), 1503(s), 1420 (w), 1368 (w), 1310 (s), 1256 (w), 1210(w), 1162 (w), 1118 (s), 1092 (s), 1000 (s), 965 (w), 913 (w), 884 (w), 788 (m), 731 (m), 677 (s), 609 (m), 513 (w), 477 (w), 421 (w).

**MOF syntheses**

Safety Note: Perchlorate salts are potentially explosive, and caution should be exercised when dealing with such materials. However, the small quantities used in this study were not found to present a hazard.

**IPA@4S,7R-CFA-22**: In a glass tube (20 mL), a solution of the respective **4S,7R-$H_3$tristmi** ligand (10 mg, 0.016 mmol) in isopropyl alcohol (2 mL) with 0.15 mL NaOH (0.1 M) was added to a solution of copper(II) perchlorate hexahydrate (25 mg, 0.07 mmol) in isopropyl alcohol (2 mL), and mixed thoroughly. The tube was closed with a plastic cap and the mixture heated at 130 °C in a heating block for three days and subsequently filtrated. **IPA@4S,7R-CFA-22** was obtained as colourless rhombohedral crystals, which were washed with methanol three times and dried under vacuum (**4S,7R-CFA-22-dry**). Yield: 10 mg (70 %); IR (v($cm^{-1}$)): 1618.05 (w), 1578.29 (m), 1495.85 (w), 1475.42 (m), 1452.53 (w), 1444.04 (w), 1414.13 (m), 1390.05 (w), 1371.08 (w), 1269.67 (w), 1237.57 (w), 1187.96 (w), 1129.22 (st), 1074.50 (st), 1055.54 (st), 916.55 (m), 883.72 (m), 839.94 (w), 798.23 (w), 708.98 (vw), 690.37 (m), 621.43 (st), 530.96 (w), 459.82 (w).

**Preparation of solvent@4S,7R-** and **solvent@4R,7S-CFA-22**

Solvent exchange was conducted on the as-synthesized single-crystals (**IPA@4S,7R- and IPA@4R,7S-CFA-22**) washed once with isopropyl alcohol and by placing them into a large excess (ca. 1mL) of the selected solvent to preserve defect-free single crystals for single-crystal analysis (**solvent@4S,7R-** and **solvent@4R,7S-CFA-22**). After exchange with fresh solvent three times over the course of at least 3 days, a complete replacement of the isopropanol molecules is assumed.

# 2. Single crystal X-ray diffraction, Structures, and Data

X-ray diffraction data for the single crystal structure determination of all compounds in this paper were collected on a Bruker D8 Venture diffractometer (Mo Kα radiation, λ = 0.71073 Å) equipped with a low-temperature device. The raw data frames were integrated and corrected for absorption effects using the Bruker SAINT[1] and SADABS[2] software packages. Structure solution by direct methods and structure refinement were performed using SHELXT 2014/5[3] and SHELXL 2018/3.[4] In most structures all non-hydrogen atoms were refined anisotropically. Hydrogen atoms were included in the final refinement cycles using a riding model with constrained $U_{iso}$ parameters.

**4S,7R-CFA-22-dry** structure was refined with a disorder of $ClO_4^-$ ion (0.45/0.55 refined ratio), which could be refined only isotropically. Multiple restrains and constraints were applied, since the diffracting ability of the crystal was very weak. Three out of four structures hosting phenylethanol revealed disorder of alcohol molecules. For the structures **rac-1-PhEtOH@4S,7R-CFA-22** and **rac-1-PhEtOH@4R,7S-CFA-22** the disorder was refined with the same occupancy of 0.45/0.55, for the structure **R-1-PhEtOH@4R,7S-CFA-22** the occupancy of disordered 1-phenylethanol molecules was set at the ratio 0.33/0.66 because of the geometrical reasons. In all three structures the AFIX constraints were applied to the phenylethanol molecules and they were refined isotropically. DFIX restrains were applied to the structures **rac-1-ButOH@4R,7S-CFA-22** and **rac-1-ButOH@4S,7R-CFA-22** with 2-buthanol and the alcohol in these structurers could not be refined anisotropically.

Except of the **CFA-22** structures with disordered 1-PhEtOH molecules (**rac-1-PhEtOH@4S,7R-CFA-22**, **rac-1-PhEtOH@4R,7S-CFA-22** and **R-1-PhEtOH@4R,7S-CFA-22**) all other structures in this paper contain possible solvent accessible voids with volumes between 371 $Å^3$ in the alcohol-free orthorhombic structure **4S,7R-CFA-22-dry** and 1361 $Å^3$ in the isopropanol containing cubic structure **IPA@4S,7R-CFA-22**. Since no additional solvent molecules could be resolved from the Fourier map, the SQUEEZE routine of PLATON[5] was applied to these structures.

All structures described in this paper crystallize in the chiral space groups. The refined Flack parameter[6] values are listed in Tables 2-4 and are close to zero for all of them, thus conforming the correct enantiopure conformation of (R/S)-camphor used in the synthesis.

Complete crystallographic data for the structures reported in this paper have been deposited as supplementary publication nos. CCDC 2282568-2282576. These data are provided free of charge from the Cambridge Crystallographic Data Centre via www.ccdc.cam.ac.uk/data_request/cif.

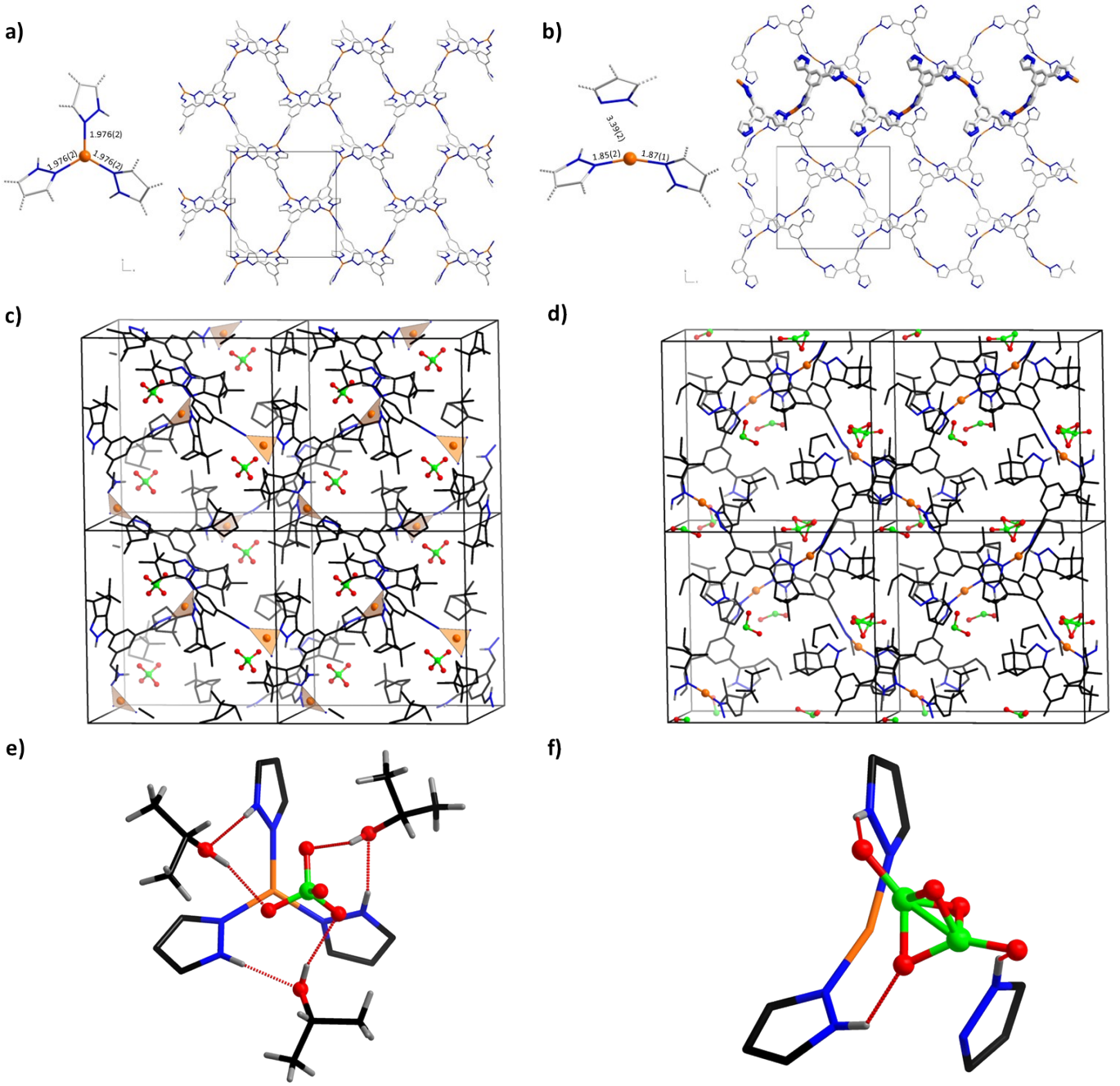


*Figure S 1:* a) SBU and network structure of as synthesized **IPA@4S,7R-CFA-22** b) showing the cleavage of one coordination bond upon drying, which results in the **4S,7R-CFA-22-dry** structure consisting of the highlighted linear chains. c) Unit cells of **IPA@4S,7R-CFA-22** and d) **4S,7R-CFA-22-dry** with solvent molecules and perchlorate anions. e) Loss of the stabilizing hydrogen-bond framework between the IPA molecules, the perchlorate anion, and the pyrazole results in f) a reversible rearrangement of the now disordered perchlorate anion in the **4S,7R-CFA-22-dry**, which causes the cleavage of one coordination bond from one pyrazole to the Cu cation.

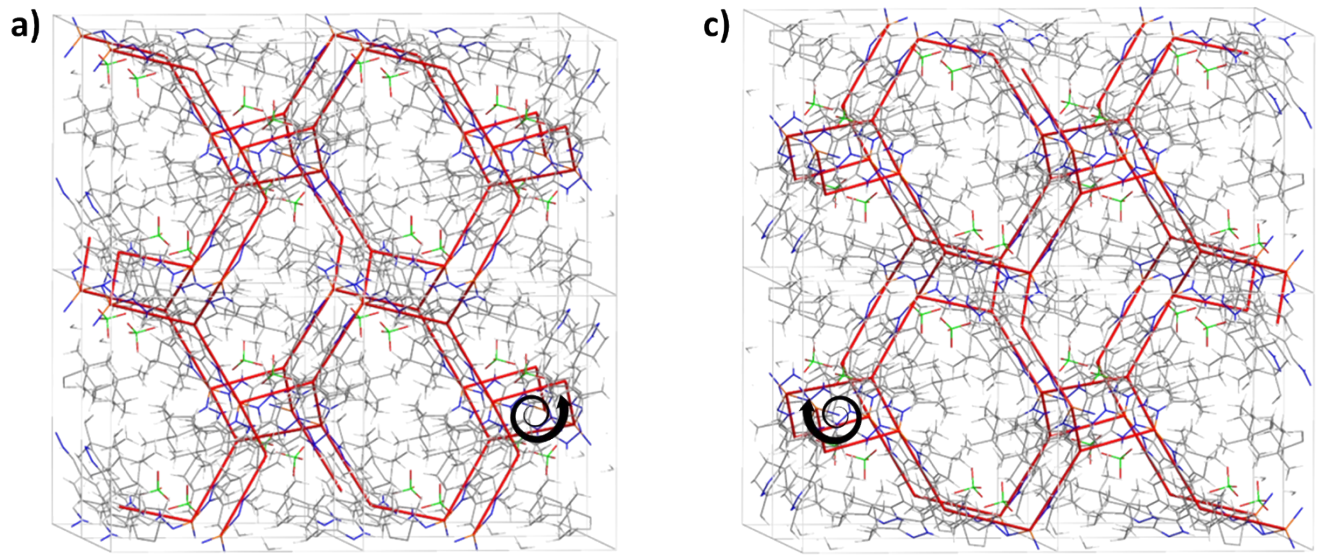


*Figure S 2:* Plots of the enantiomeric a) **rac-1-PhEtOH@4S,7R-CFA-22** and b) **rac-1-PhEtOH@4R,7S-CFA-22** structures without solvent molecules showing the different rotation of the spirals in the frameworks srs-topology.

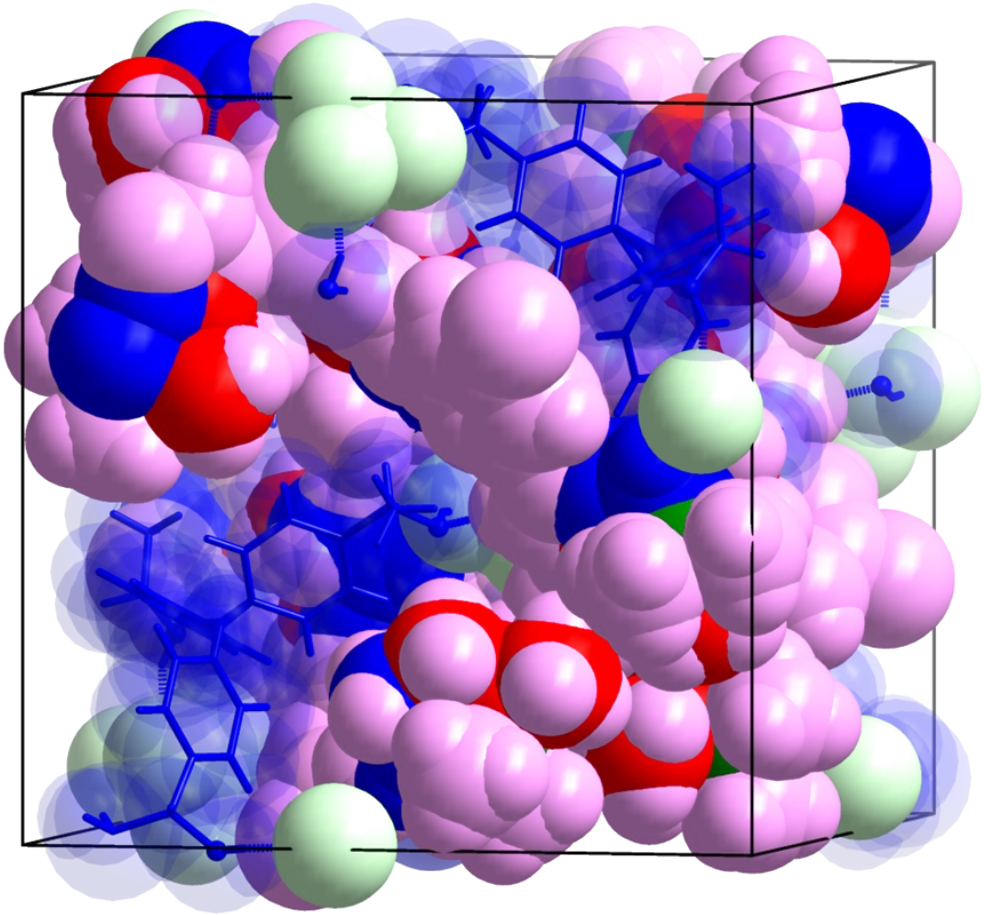

*Figure S 3:* Space filling plot of the **R-1-PhEtOH@4R,7S-CFA-22** framework and $ClO_4^-$ counter ions (light green) showing the arrangement of the R-1-PhEtOH guest molecules (blue in pink) with the 33% occupancy, as well as the frameworks R (blue) and S stereocenters (red).

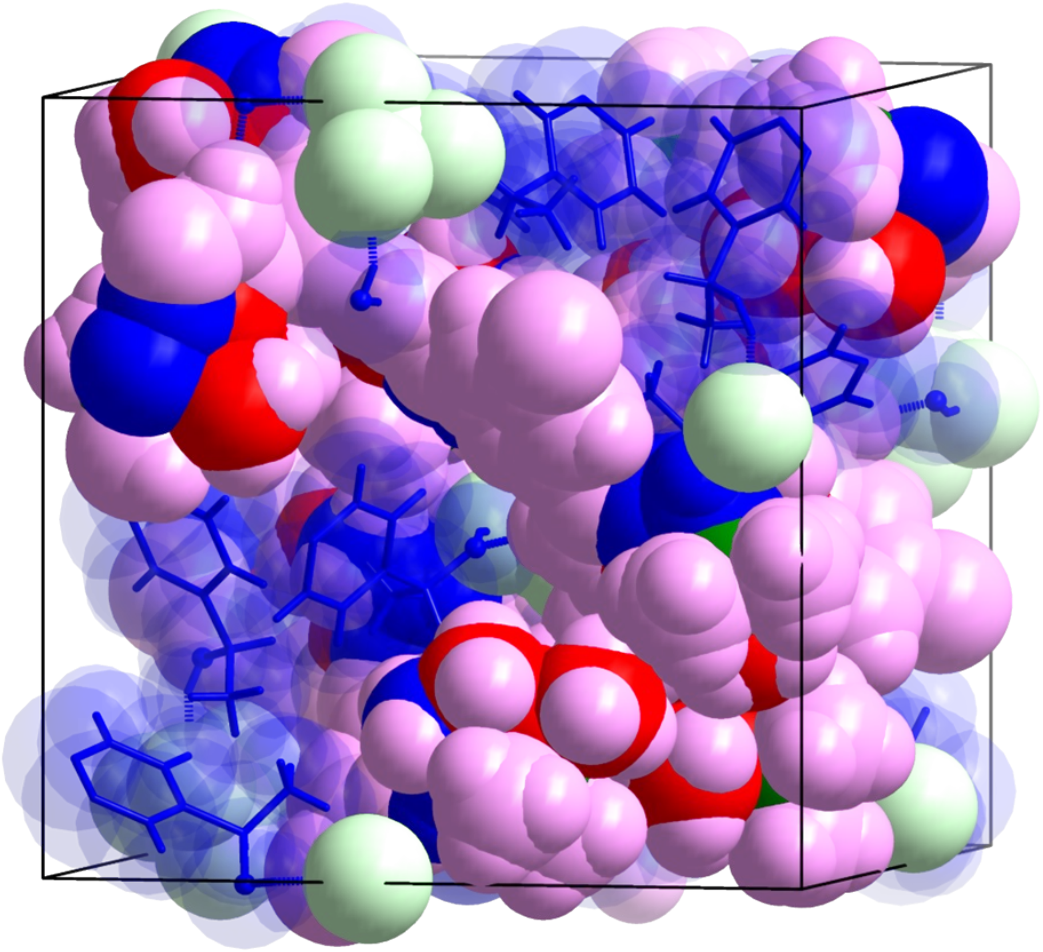

*Figure S 4:* Space filling plot of the **R-1-PhEtOH@4R,7S-CFA-22** framework and $ClO_4^-$ counter ions (light green) showing the arrangement of the R-1-PhEtOH guest molecules (blue in pink) with the 67% occupancy, as well as the frameworks R (blue) and S stereocenters (red).

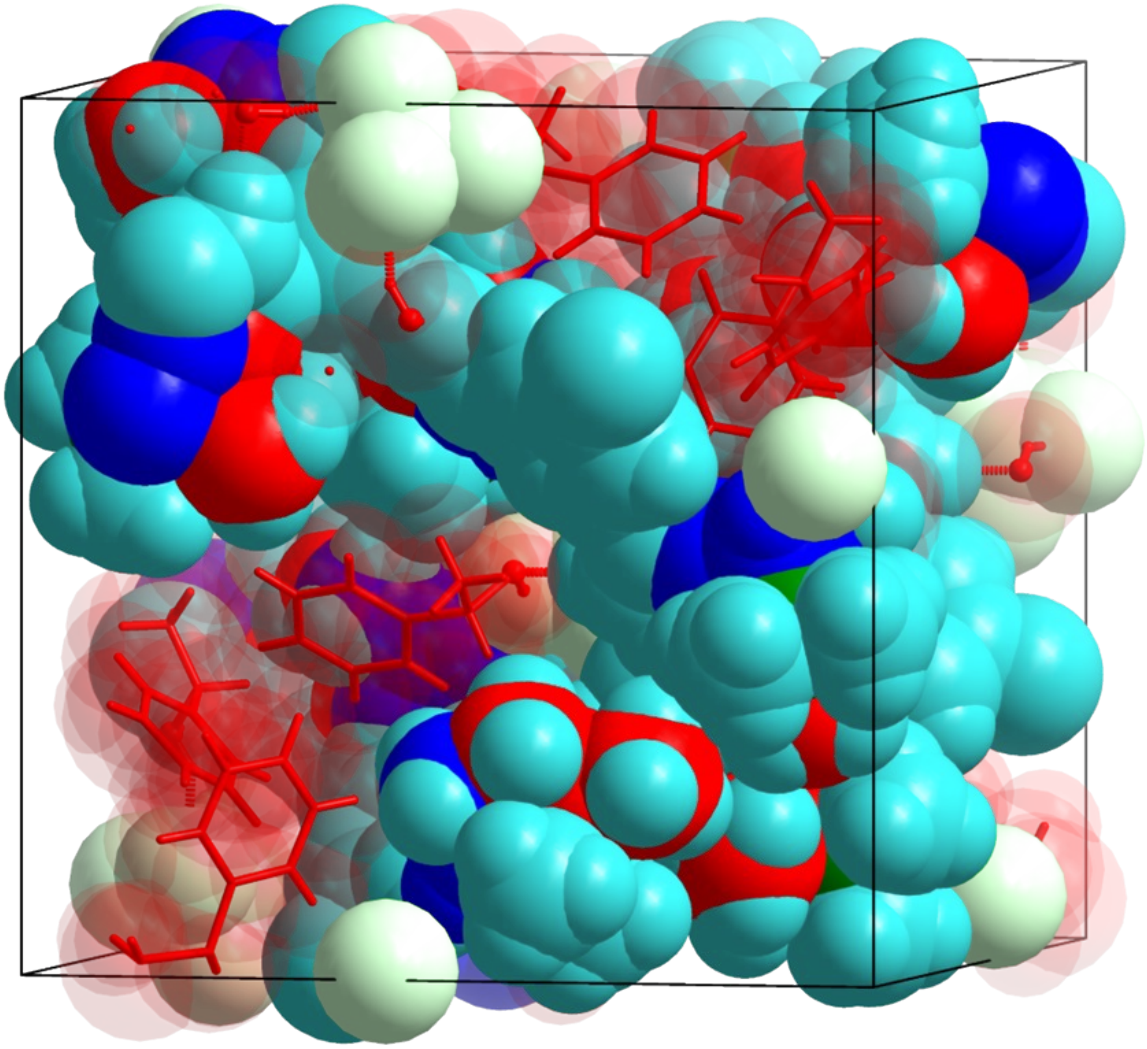

*Figure S 5:* Space filling plot of the **S-1-PhEtOH@4R,7S-CFA-22** framework and $ClO_4^-$ counter ions (light green) showing the arrangement of the S-1-PhEtOH guest molecules (red in turquoise), as well as the frameworks R (blue) and S stereocenters (red).

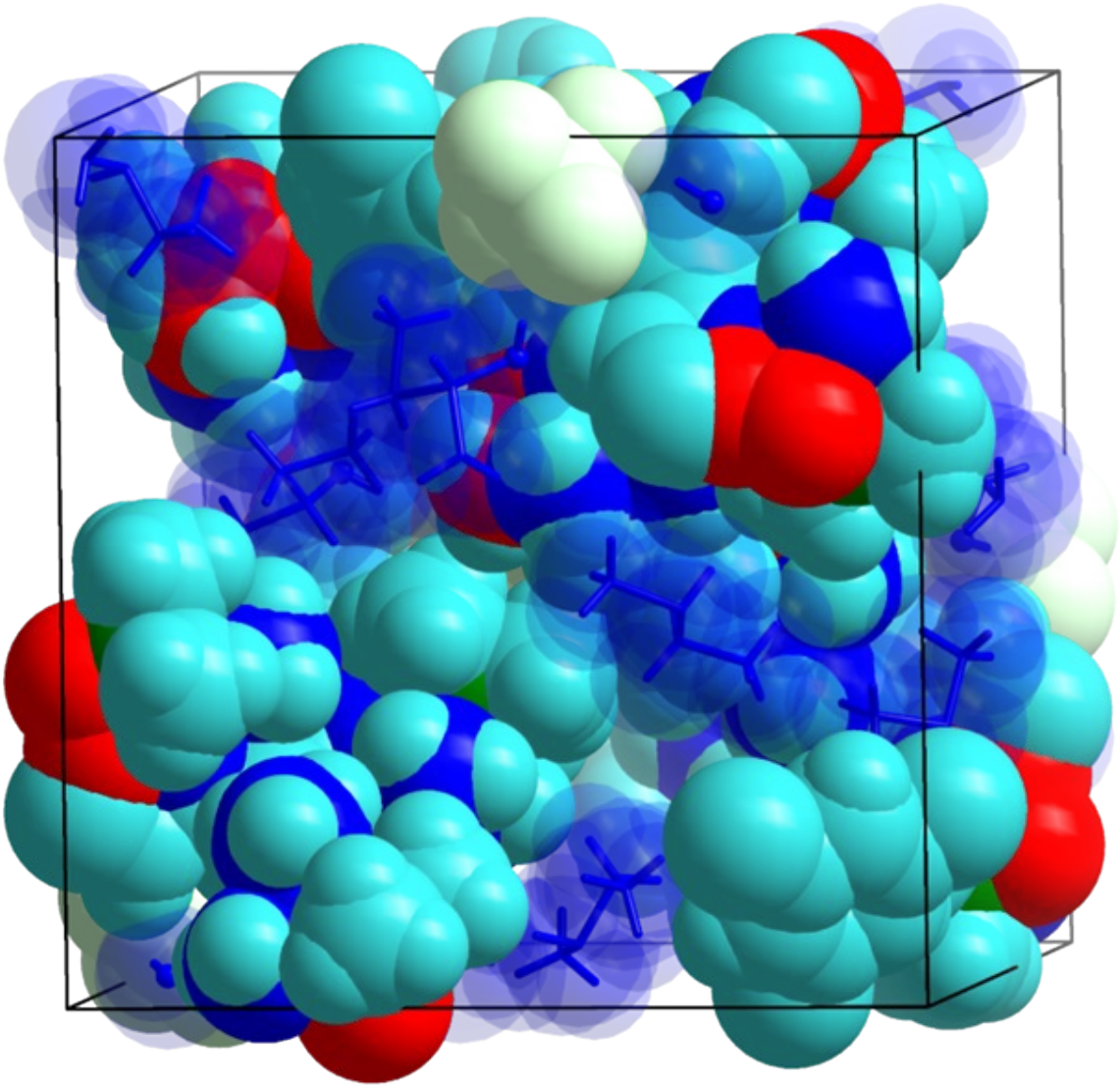

*Figure S 6:* Space filling plots of the **rac-2-ButOH@4R,7S-CFA-22** framework and $ClO_4^-$ counter ions (light green) showing the arrangement of the S-2-ButOH guest molecules (blue in turquoise), as well as the frameworks R (blue) and S stereocenters (red).

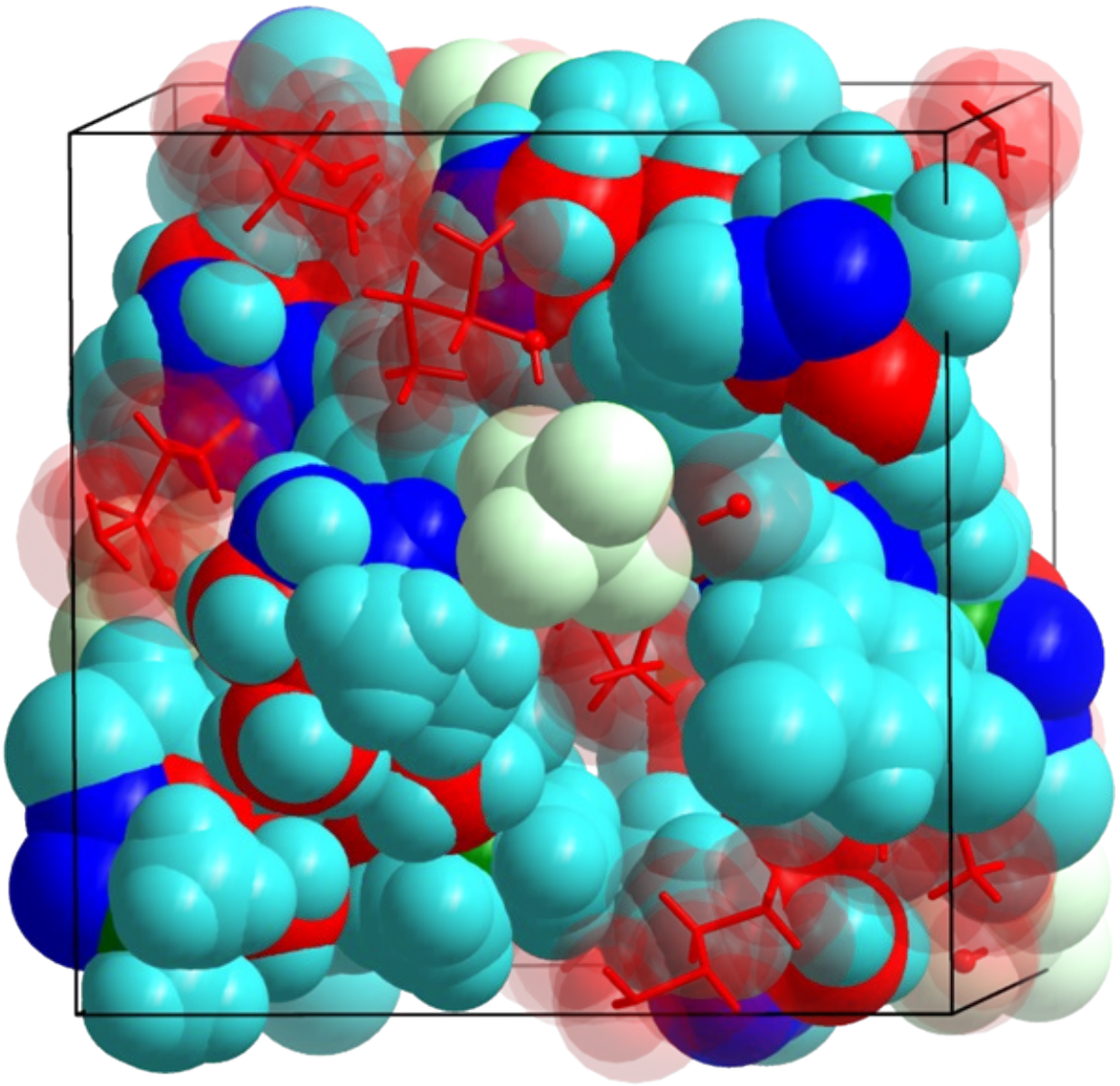

*Figure S 7:* Space filling plots of the **rac-2-ButOH@4S,7R-CFA-22** framework and $ClO_4^-$ counter ions (light green) showing the arrangement of the R-2-ButOH guest molecules (red in turquoise), as well as the frameworks R (blue) and S stereocenters (red).

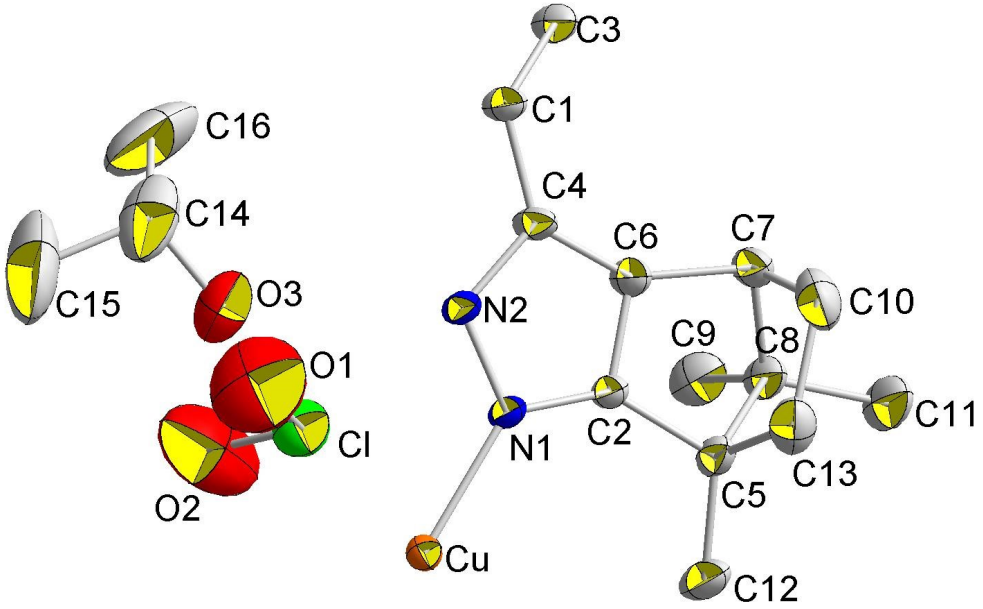


*Figure S 8:* ORTEP-Style plot of **IPA@4S,7R-CFA-22**.

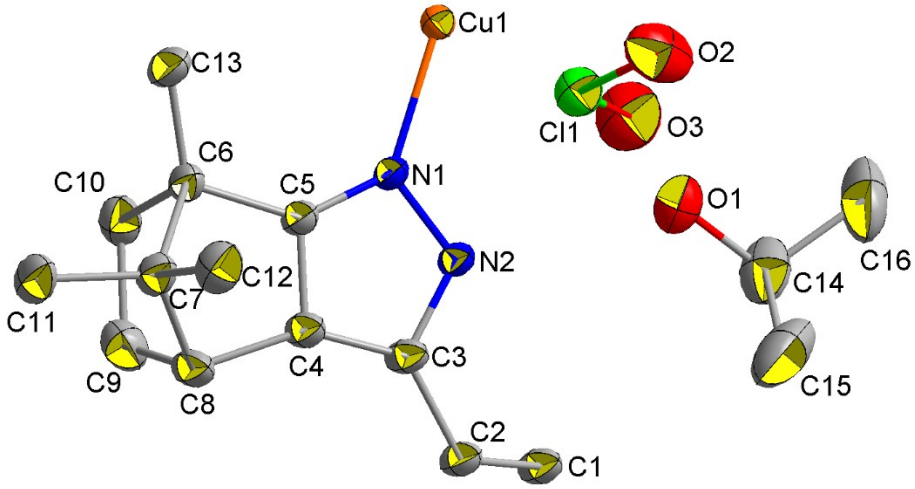


*Figure S 9:* ORTEP-Style plot of **IPA@4R,7S-CFA-22**

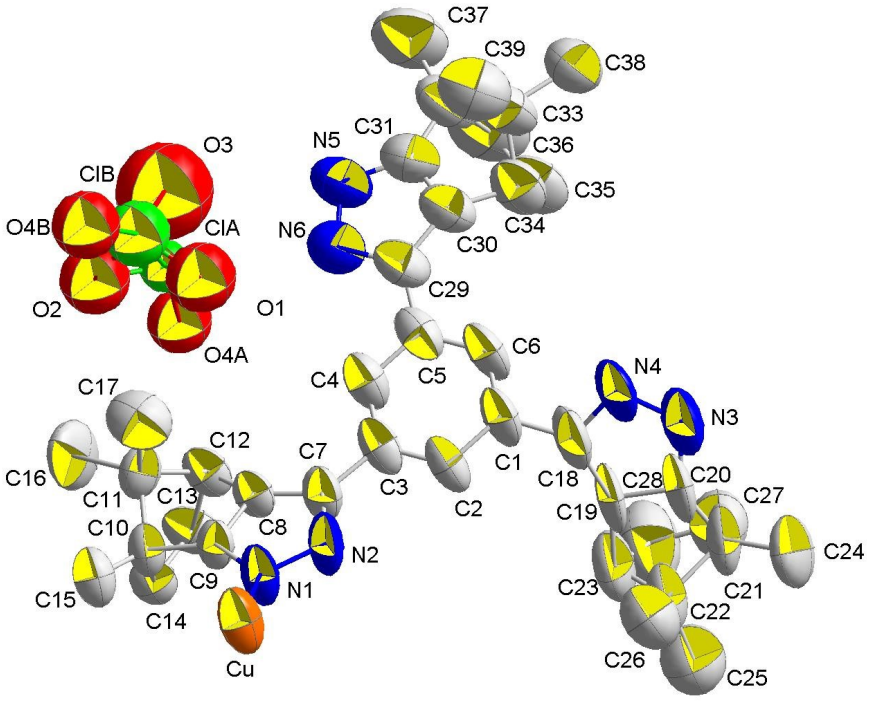


*Figure S 10:* ORTEP-Style plot of **4S,7R-CFA-22-dry**.

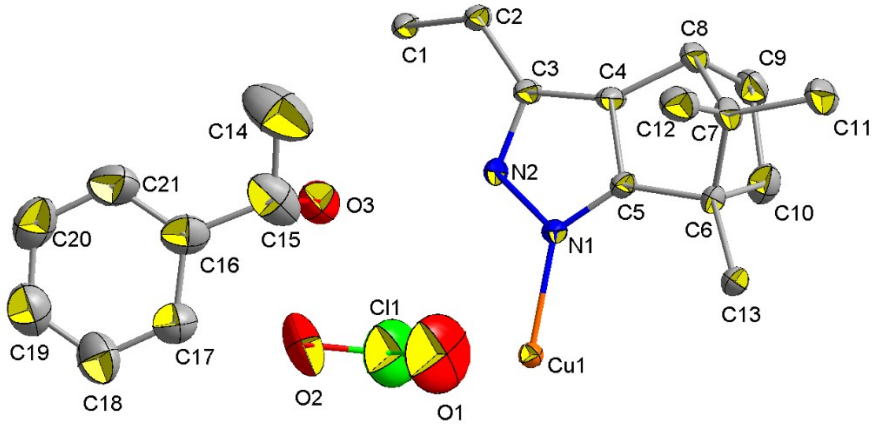


*Figure S 11:* ORTEP-Style plot of **S-1-PhEtOH@4R,7S-CFA-22**

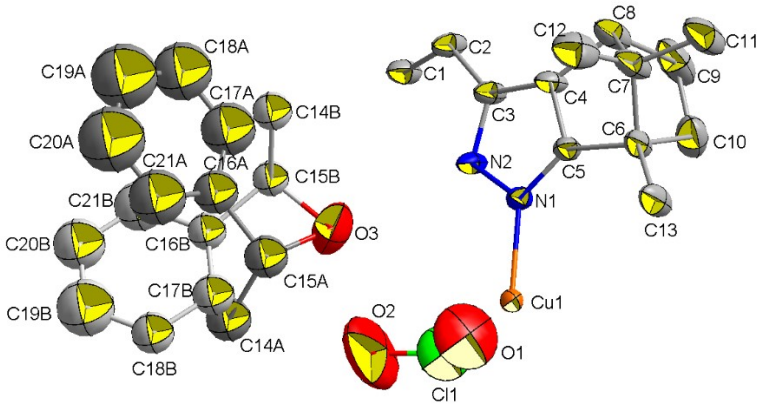


*Figure S 12:* ORTEP-Style plot of **R-1-PhEtOH@4R,7S-CFA-22**

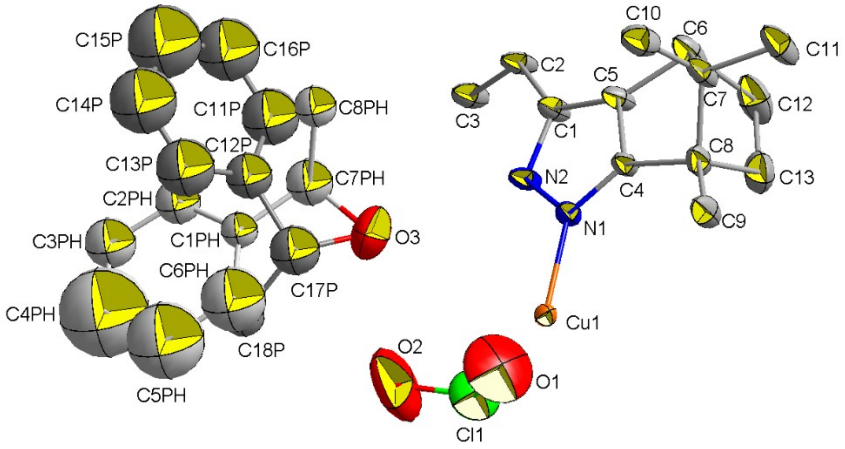


*Figure S 13:* ORTEP-Style plot of **rac-1-PhEtOH@4R,7S-CFA-22**

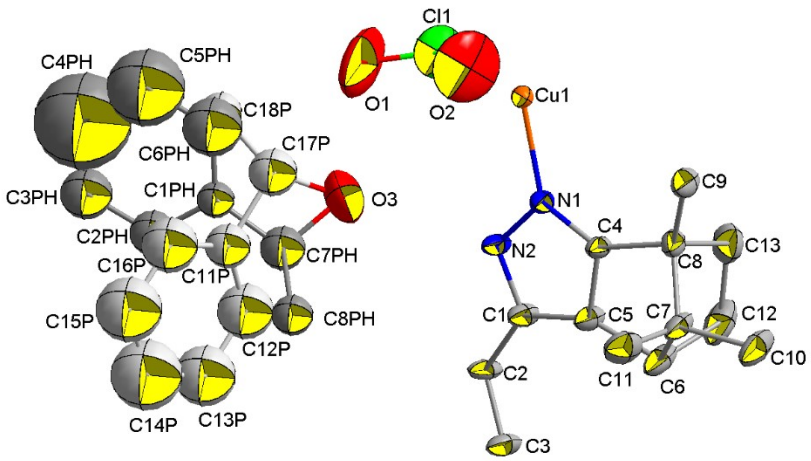


*Figure S 14:* ORTEP-Style plot of **rac-1-PhEtOH@4S,7R-CFA-22**

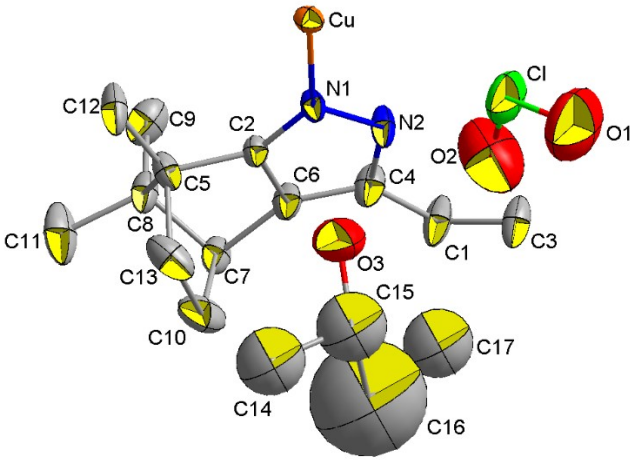


*Figure S 15:* ORTEP-Style plot of **rac-2-ButOH@4S,7R-CFA-22**

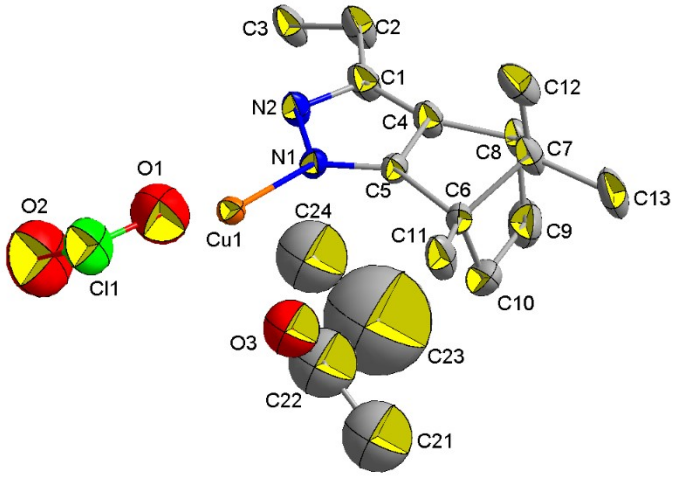


*Figure S 16:* ORTEP-Style plot of **rac-2-ButOH@4R,7S-CFA-22**

Table S1. Crystal Data and Structural Refinement for **IPA@4S,7R-CFA-22**, **IPA@4R,7S-CFA-22**, and **4S,7R-CFA-22-dry.**

| **Compound**[1] | **IPA@4S,7R-CFA-22** | **IPA@4R,7S-CFA-22** | **4S,7R-CFA-22-dry** |
|---|---|---|---|
| file | mo_ks488b_0m_a_sq_publ2 | mo_rr588b_isop_0m_a_sq | mo_ks540a_7_0m_a_sq_publ |
| empirical formula | $C_{48}H_{72}ClCuN_6O_7$ | $C_{48}H_{72}ClCuN_6O_7$ | $C_{39}H_{48}ClCuN_6O_4$ |
| formula | $[Cu(C_{39}H_{48}N_6)(ClO_4)]\cdot 3(C_3H_8O)$ | $[Cu(C_{39}H_{48}N_6)(ClO_4)]\cdot 3(C_3H_8O)$ | $[Cu(C_{39}H_{48}N_6)(ClO_4)]$ |
| formula weight (g mol$^{-1}$) | 944.10 | 944.10 | 763.82 |
| temperature (K) | 250(2) | 150(2) | 200(2) |
| wavelength (Å) | 0.71073 | 0.71073 | 0.71073 |
| crystal system | Cubic | Cubic | Orthorhombic |
| space group | $P2_13$ | $P2_13$ | $P2_12_12_1$ |
| *a* (Å) | a = 18.0217(3) | a = 17.9422(4) | a = 11.5467(12) |
| *b* (Å) | -"- | -"- | b = 17.9284(18) |
| *c* (Å) | -"- | -"- | c = 19.841(2) |
| volume (Å$^3$) | 5853.1(3) | 5776.0(4) | 4107.4(7) |
| *Z* | 4 | 4 | 4 |
| $D_g$ (g cm$^{-3}$) | 1.071 | 1.086 | 1.235 |
| μ (mm$^{-1}$) | 0.465 | 0.471 | 0.641 |
| *F*(000) | 2016 | 2016 | 1608 |
| crystal size (mm$^3$) | 0.1 x 0.1 x 0.1 | 0.04 x 0.04 x 0.04 | 0.07 x 0.04 x 0.02 |
| Θ range (°) | 2.527 to 27.245. | 2.270 to 27.458 | 2.272 to 18.864 |
| reflections collected | 52439 | 94562 | 26992 |
| independent reflections | 4388 [R(int) = 0.0646] | 4423 [R(int) = 0.0627] | 3244 [R(int) = 0.1162] |
| Completeness (%) | 99.8 | 99.8 | 99.8 |
| data/restraints/parameters | 4388 / 0 / 196 | 4423 / 0 / 196 | 3244 / 568 / 414 |
| goodness of fit on $F^2$ | 1.043 | 1.058 | 1.055 |
| final R indices [$I$ > 2sigma($I$)] | R1 = 0.0390, wR2 = 0.0949 | R1 = 0.0339, wR2 = 0.0874 | R1 = 0.1241, wR2 = 0.3243 |
| R indices (all data) | R1 = 0.0481, wR2 = 0.0989 | R1 = 0.0385, wR2 = 0.0903 | R1 = 0.1529, wR2 = 0.3559 |
| Absolute structure parameter | 0.020(5) | -0.003(4) | 0.03(2) |
| largest diff. peak and hole/e.Å$^{-3}$ | 0.590 and -0.301 | 0.371 and -0.346 | 0.654 and -0.314 |
| CCDC No. | 2282570 | 2282573 | 2282569 |

Table S2. Crystal Data and Structural Refinement for **S-1-PhEtOH@4R,7S-CFA-22**, **R-1-PhEtOH@4R,7S-CFA-22**, **rac-1-PhEtOH@4R,7S-CFA-22**, and **rac-1-PhEtOH@4S,7R-CFA-22.**

| **Compound**[j] | **S-1-PhEtOH@4R,7S-CFA-22** | **R-1-PhEtOH@4R,7S-CFA-22** | **rac-1-PhEtOH @4R,7S-CFA-22** | **rac-1-PhEtOH @4S,7R-CFA-22** |
|---|---|---|---|---|
| file | mo_rr588b_rph_0m_a_sq | mo_RR588b_RPhE_0m_a | mo_KSPhEth_0m_a | mo_KS586_0m_a |
| empirical formula | $C_{63}H_{78}ClCuN_6O_7$ | $C_{63}H_{78}ClCuN_6O_7$ | $C_{63}H_{78}ClCuN_6O_7$ | $C_{63}H_{78}ClCuN_6O_7$ |
| formula | $[Cu(C_{39}H_{48}N_6)(ClO_4)]\cdot3(C_8H_{10}O)$ | $[Cu(C_{39}H_{48}N_6)(ClO_4)]\cdot3(C_8H_{10}O)$ | $[Cu(C_{39}H_{48}N_6)(ClO_4)]\cdot3(C_8H_{10}O)$ | $[Cu(C_{39}H_{48}N_6)(ClO_4)]\cdot3(C_8H_{10}O)$ |
| formula weight (g $mol^{-1}$) | 1130.30 | 1130.30 | 1130.30 | 1130.30 |
| temperature (K) | 150(2) | 150(2) | 150(2) | 150(2) |
| wavelength (Å) | 0.71073 | 0.71073 | 0.71073 | 0.71073 |
| crystal system | Cubic | Cubic | Cubic | Cubic |
| space group | $P2_13$ | $P2_13$ | $P2_13$ | $P2_13$ |
| *a* (Å) | a = 18.3042(2) | a = 18.2310(2) | a = 18.2489(2) | a = 18.2443(3) |
| volume ($Å^3$) | 6132.7(2) | 6059.4(2) | 6077.3(2) | 6072.7(3) |
| *Z* | 4 | 4 | 4 | 4 |
| $D_g$ (g $cm^{-3}$) | 1.224 | 1.239 | 1.235 | 1.236 |
| μ ($mm^{-1}$) | 0.455 | 0.461 | 0.459 | 0.460 |
| *F*(000) | 2400 | 2400 | 2400 | 2400 |
| crystal size ($mm^3$) | 0.07 x 0.07 x 0.07 | 0.07 x 0.06 x 0.06 | 0.08 x 0.08 x 0.08 | 0.08 x 0.08 x 0.06 |
| Θ range (°) | 2.488 to 26.978 | 2.234 to 27.496 | 2.232 to 27.493 | 2.233 to 26.479 |
| reflections collected | 21202 | 46324 | 73245 | 161438 |
| independent reflections | 4482 [R(int) = 0.0522] | 4654 [R(int) = 0.0455] | 4660 [R(int) = 0.0426] | 4202 [R(int) = 0.0570] |
| Completeness (%) | 99.9 | 99.8 | 99.8 | 99.8 |
| data/restraints/parameters | 4482 / 6 / 240 | 4654 / 6 / 208 | 4660 / 6 / 209 | 4202 / 6 / 209 |
| goodness of fit on $F^2$ | 1.042 | 1.086 | 1.075 | 1.069 |
| final R indices [$I$ > 2sigma($I$)] | R1 = 0.0701, wR2 = 0.1848 | R1 = 0.0723, wR2 = 0.1995 | R1 = 0.0775, wR2 = 0.2099 | R1 = 0.0760, wR2 = 0.2049 |
| R indices (all data) | R1 = 0.0810, wR2 = 0.1952 | R1 = 0.0776, wR2 = 0.2056 | R1 = 0.0805, wR2 = 0.2135 | R1 = 0.0786, wR2 = 0.2082 |
| Absolute structure parameter | 0.014(8) | 0.005(5) | 0.018(5) | 0.010(4) |
| largest diff. peak and hole/e.$Å^{-3}$ | 1.309 and -0.862 | 1.025 and -0.978 | 1.092 and -1.081 | 0.911 and -0.983 |
| CCDC No. | 2282568 | 2282572 | 2282576 | 2282574 |

Table S3. Crystal Data and Structural Refinement for **rac-2-ButOH@4S,7R-CFA-22** and **rac-2-ButOH@4R,7S-CFA-22.**

| **Compound**[j] | **rac-2-ButOH@4S,7R-CFA-22** | **rac-2-ButOH@4R,7S-CFA-22** |
|---|---|---|
| file | mo_ks571a_0m_a_sq_final | mo_ks2bu_2_0m_a_sq_final2 |
| empirical formula | $C_{51}H_{78}ClCuN_6O_7$ | $C_{51}H_{78}ClCuN_6O_7$ |
| formula | $[Cu(C_{39}H_{48}N_6)(ClO_4)]\cdot 3(C_4H_{10}O)$ | $[Cu(C_{39}H_{48}N_6)(ClO_4)]\cdot 3(C_4H_{10}O)$ |
| formula weight (g $mol^{-1}$) | 986.18 | 986.18 |
| temperature (K) | 150(2) | 150(2) |
| wavelength (Å) | 0.71073 | 0.71073 |
| crystal system | Cubic | Cubic |
| space group | $P2_13$ | $P2_13$ |
| *a* (Å) | a = 18.0076(3) | a = 18.0116(2) |
| volume ($Å^3$) | 5839.4(3) | 5843.28(19) |
| *Z* | 4 | 4 |
| $D_g$ (g $cm^{-3}$) | 1.122 | 1.121 |
| μ ($mm^{-1}$) | 0.468 | 0.468 |
| *F*(000) | 2112 | 2112 |
| crystal size ($mm^3$) | 0.12 x 0.09 x 0.07 | 0.16 x 0.14 x 0.14 |
| Θ range (°) | 2.262 to 26.993 | 2.261 to 27.480 |
| reflections collected | 157489 | 101222 |
| independent reflections | 4251 [R(int) = 0.0520] | 4488 [R(int) = 0.0369] |
| Completeness (%) | 99.8 | 99.8 |
| data/restraints/parameters | 4251 / 9 / 185 | 4488 / 10 / 180 |
| goodness of fit on $F^2$ | 1.051 | 1.048 |
| final R indices [$I > 2\text{sigma}(I)$] | R1 = 0.0698, wR2 = 0.1912 | R1 = 0.0727, wR2 = 0.2028 |
| R indices (all data) | R1 = 0.0717, wR2 = 0.1940 | R1 = 0.0753, wR2 = 0.2069 |
| Absolute structure parameter | 0.012(5) | 0.015(5) |
| largest diff. peak and hole/e.$Å^{-3}$ | 1.259 and -0.663 | 1.449 and -0.778 |
| CCDC No. | 2282575 | 2282571 |

Table S4. SQUEEZE data and the resulting additional non-refined solvent molecules per formula unit for **IPA@4S,7R-CFA-22**, **IPA@4R,7S-CFA-22**, **4S,7R-CFA-22-dry**, **S-1-PhEtOH@4R,7S-CFA-22**, **R-1-PhEtOH@4R,7S-CFA-22**, **rac-1-PhEtOH@4R,7S-CFA-22**, **rac-1-PhEtOH@4S,7R-CFA-22, rac-2-ButOH@4S,7R-CFA-22** and **rac-2-ButOH@4R,7S-CFA-22 (Data Squeezed without refined solvent molecules)**

| **Compound**[1] | **IPA@4S,7R-CFA-22** | **IPA@4R,7S-CFA-22** | **4S,7R-CFA-22-dry** | **S-1-PhEtOH@4R,7S-CFA-22** | **R-1-PhEtOH@4R,7S-CFA-22** | **rac-1-PhEtOH@4R,7S-CFA-22** | **rac-1-PhEtOH@4S,7R-CFA-22** | **rac-2-ButOH@4S,7R-CFA-22** | **rac-2-ButOH@4R,7S-CFA-22** |
|---|---|---|---|---|---|---|---|---|---|
| solvent accessible void volume, Å$^3$ | 1361 | 1317 | 371 | 881 / 3025 | 77 / 2963 | 128 / 2980 | 126 / 2978 | 1149 | 1134 |
| electron count Voids / cell | 193 | 238 | 46 | 202 / 925 | 10 / 717 | 6 / 743 | 6 / 720 | 194 | 212 |
| additional solvent molecules / cell | 5.68 | 7 | 1.35 | 3.06 | 0.15 | 0.09 | 0.09 | 4.62 | 5.05 |
| total solvent molecules / cell | 17.68 | 19 | 1.35 | 15.06 / 14.01 | 12.15 / 10.86 | 12.09 / 11.26 | 12.09 / 10.91 | 16.62 | 17.05 |
| solvent mass% | 58.17 | 59.92 | 9.6 | 70.66 | 66.02 | 65.91 | 65.91 | 61.72 | 62.32 |

# 3. 1-Phenylethanol Enantiomer Separation and High-Performance Liquid Chromatography (HPLC) Experiments

To determine the enantiomer ratio of 1-phenylethanol adsorbed into the pores of **rac-1-PhEtOH@4S,7R-CFA-22**, a fresh sample of **CFA-22** (approximately 8-10 mg) was transferred into a small glass vial, washed via decantation with isopropyl alcohol (3 x 2 mL), and subsequently the solvent exchanged with 1-phenylethanol (3 x 0.5 mL) over the course of one day. The sample was left for four days at ambient conditions and the 1-phenylethanol removed with a pipette. To remove residual 1-phenylethanol between the crystals, the sample was quickly washed with n-heptane (2 x 1 mL) via decantation and left to dry. The dry crystals were refilled into a fresh glass vial and washed with n-heptane (1 x 1 mL) again, before the 1-phenylethanol was washed out by soaking the crystals in isopropyl alcohol (0.1 mL) overnight. The sample was then filtered through a 0.2 µm PTFE syringe filter and washed with n-heptane (0.4 mL).

To determine the enantiomer ratio of 1-phenylethanol adsorbed into the pores of **rac-1-PhEtOH@4R,7S-CFA-22**, a fresh sample of **CFA-22** (approximately 8-10 mg) was transferred into a small glass vial, washed via decantation with isopropyl alcohol (3 x 2 mL), and subsequently the solvent exchanged with 1-phenylethanol (3 x 0.5 mL) over the course of one day. The sample was left for four days at ambient conditions and the 1-phenylethanol removed via filtration. To remove leftover 1-phenylethanol between the crystals, they were dried under vacuum for several minutes until a non-sticking powder was obtained. The 1-phenylethanol was washed out by soaking the crystals in an n-heptane/isopropyl alcohol solution (0.5 mL) overnight. The sample was then filtered through a 0.2 µm PTFE syringe filter.

The resulting solutions, as well as the racemate were analysed with a Hitachi LaChrom Elite® HPLC System (L-2455 diode array detector; L-2300 column oven; L-2200 autosampler; L-2130 pump) equipped with a Daicel CHIRALCEL® OD-H (4.6 x 250 mm; 5 µm) column and applying an n-heptane/isopropyl alcohol (97:3) mobile phase with a 0.08-0.1 $mLmin^{-1}$ flow rate and signal detection at 208 nm.

Enantiomeric excess values in percent were calculated from the HPLC chromatogram areas according to the general formula: $ee\% = \frac{A_{excess} - A_{deficient}}{A_{excess} + A_{deficient}} \times 100$ .

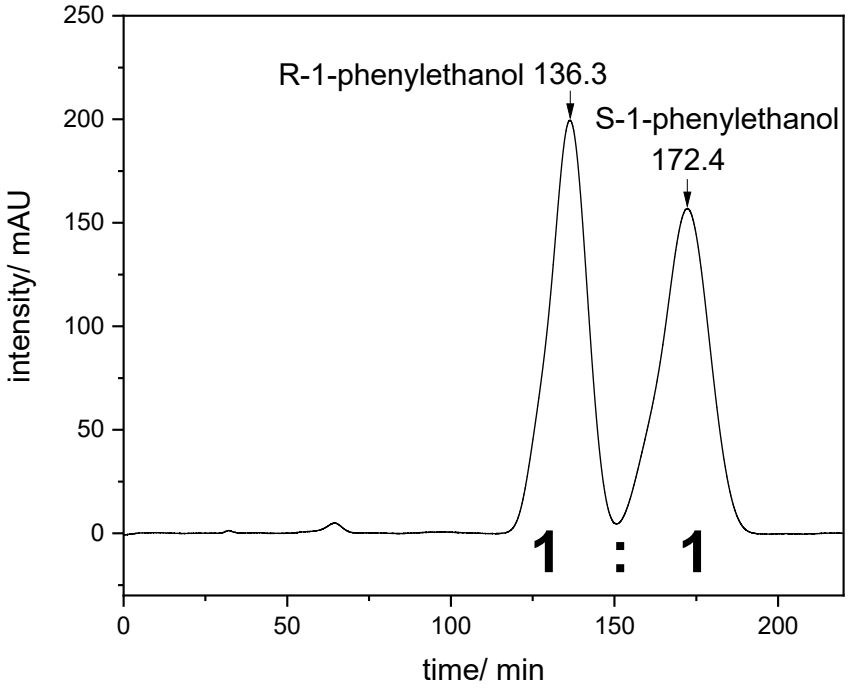


*Figure S 17:* HPLC chromatogram obtained for racemic 1-phenylethanol

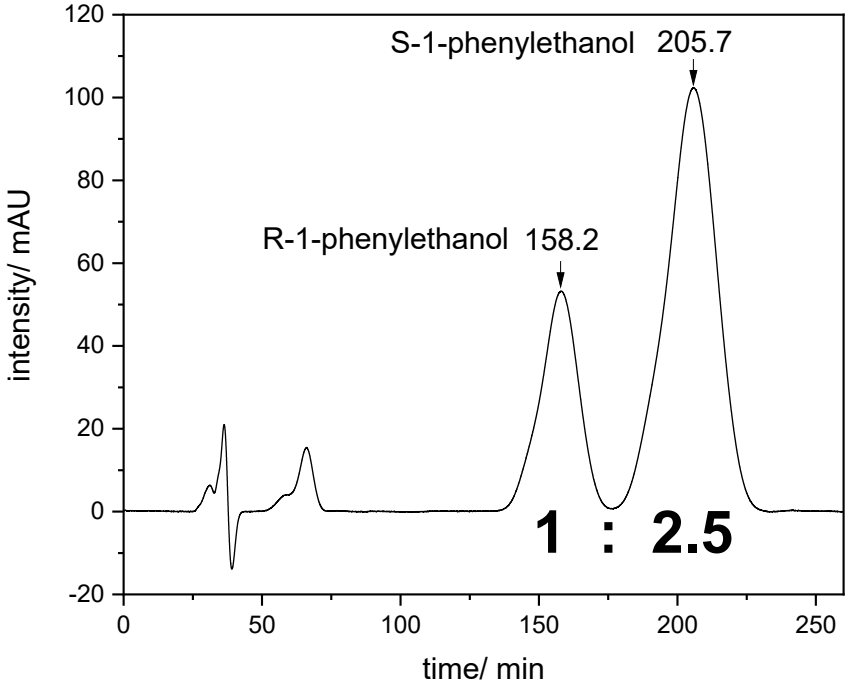


*Figure S 18:* HPLC chromatogram obtained for the 1-phenylethanol extracted from rac-1-PhEtOH@4S,7R-CFA-22.

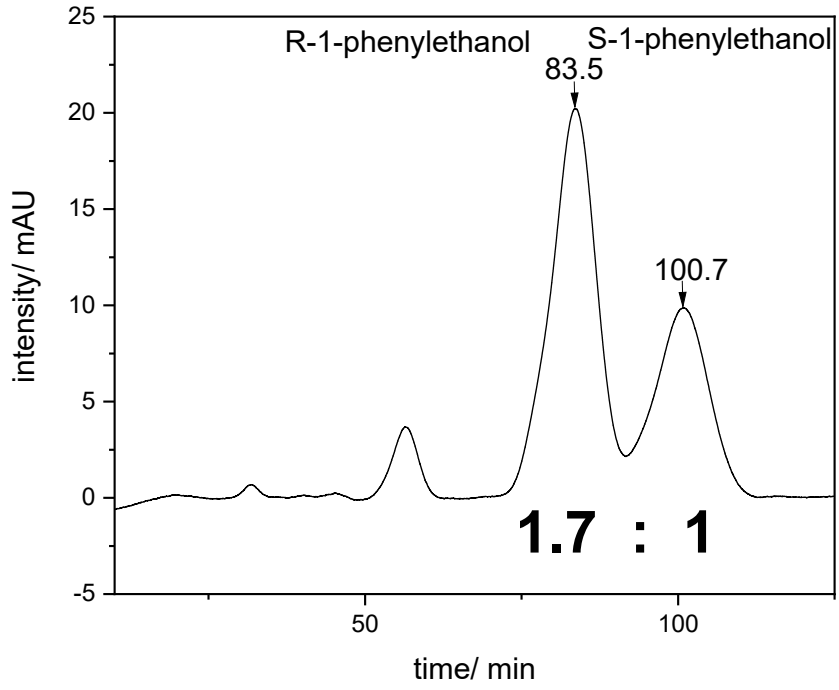


*Figure S 19:* HPLC chromatogram obtained for the 1-phenylethanol extracted from **rac-1-PhEtOH@4R,7S-CFA-22.**

# 4. NMR and HR Mass Spectroscopy

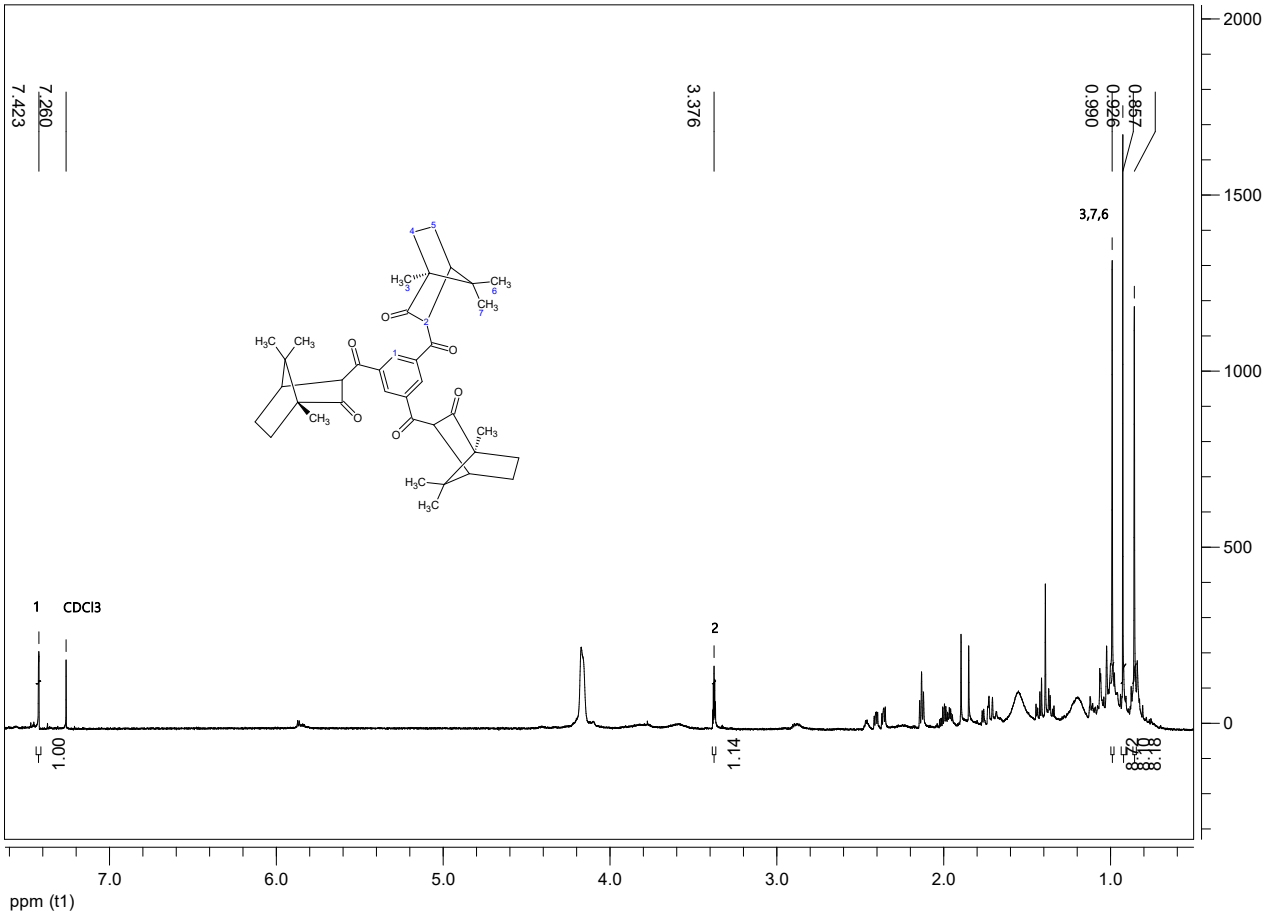


*Figure S 20:* $^1$H-NMR of compound **R-2** (400 MHz, $CDCl_3$:MeOD = 5:1, 20°C).

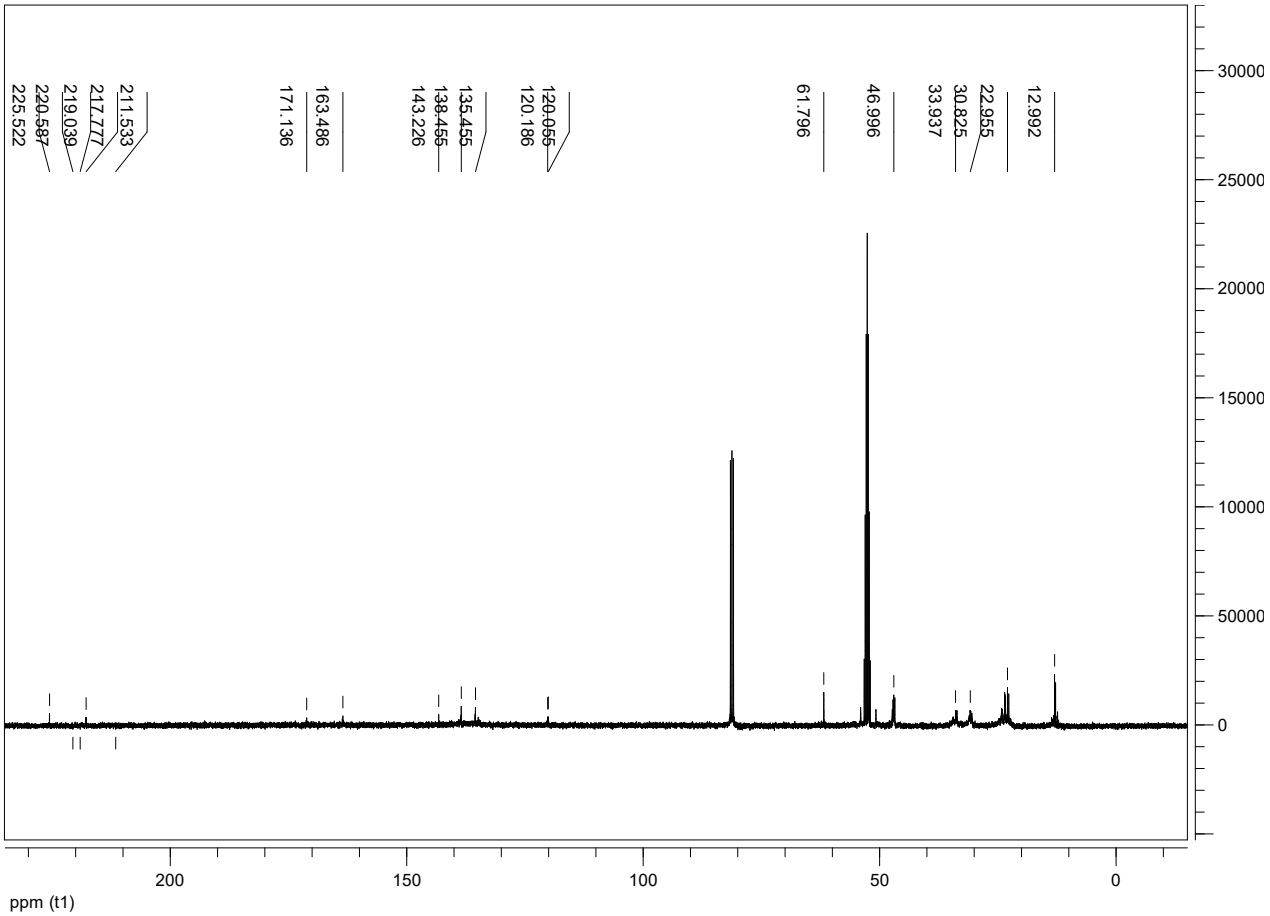


*Figure S 21:* $^{13}$C-NMR of compound **R-2** (400 MHz, $CDCl_3$:MeOD = 5:1, 20°C).

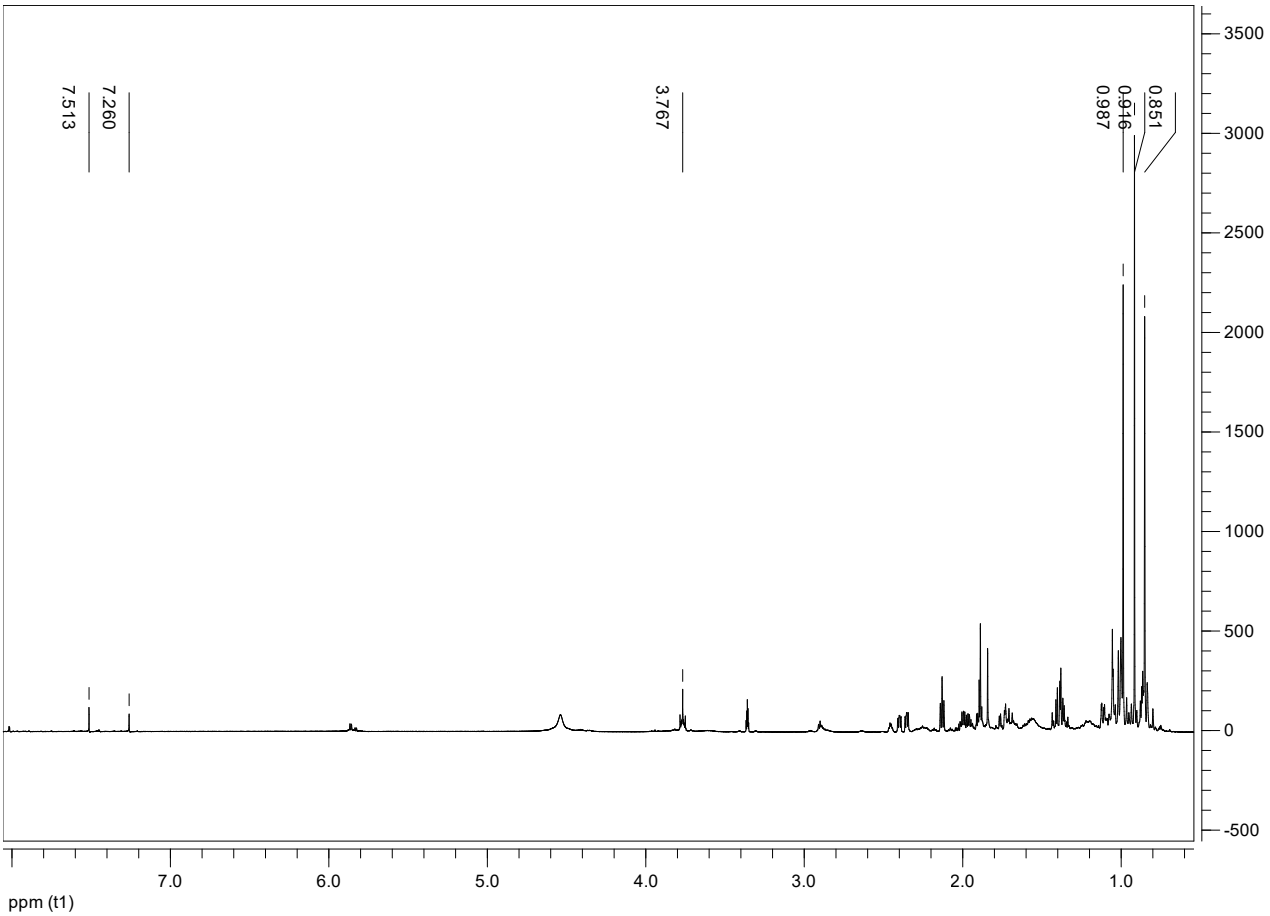


*Figure S 22:* $^{1}$H-NMR of **S-2** (400 MHz, $CDCl_3$:MeOD = 5:1, 20°C).

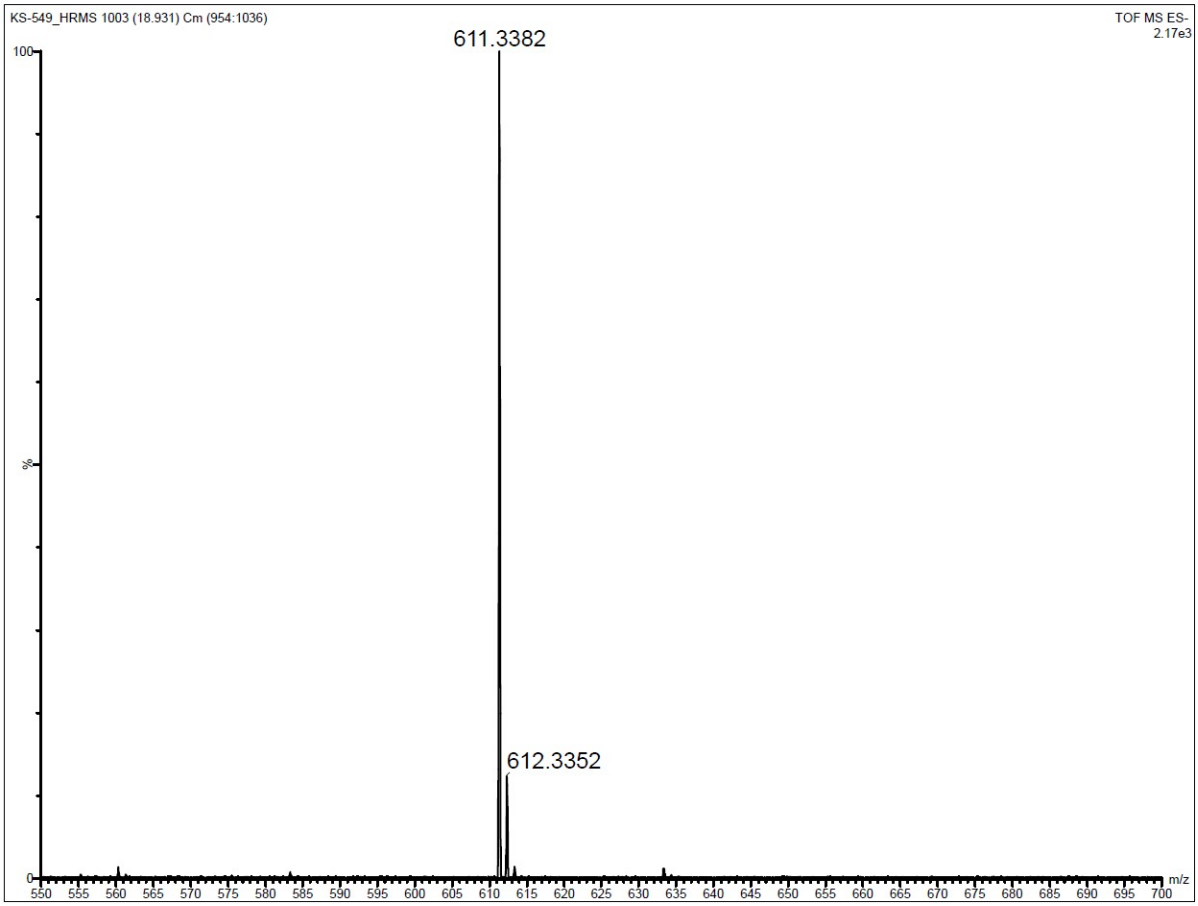


*Figure S 23:* HR-ESI(-)-MS of compound **R-2***;* $[C_{39}H_{48}O_6 - H^-]^-$ requires 611.3378; found m/z 611.3382.

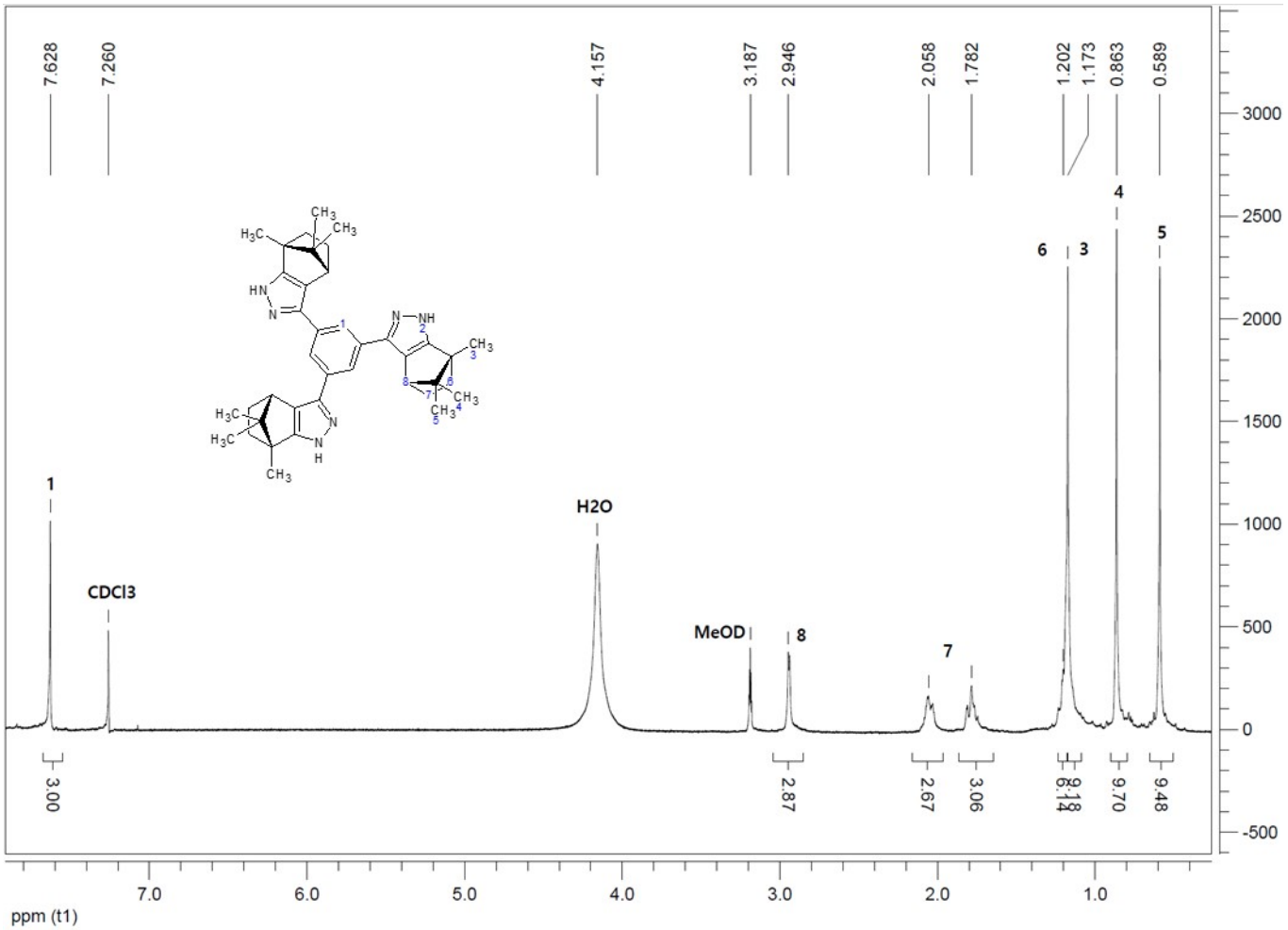


*Figure S 24:* $^{1}$H-NMR of the **4S,7R-H$_3$tristmi** ligand (400 MHz, $CDCl_3$:MeOD = 5:1, 20°C).

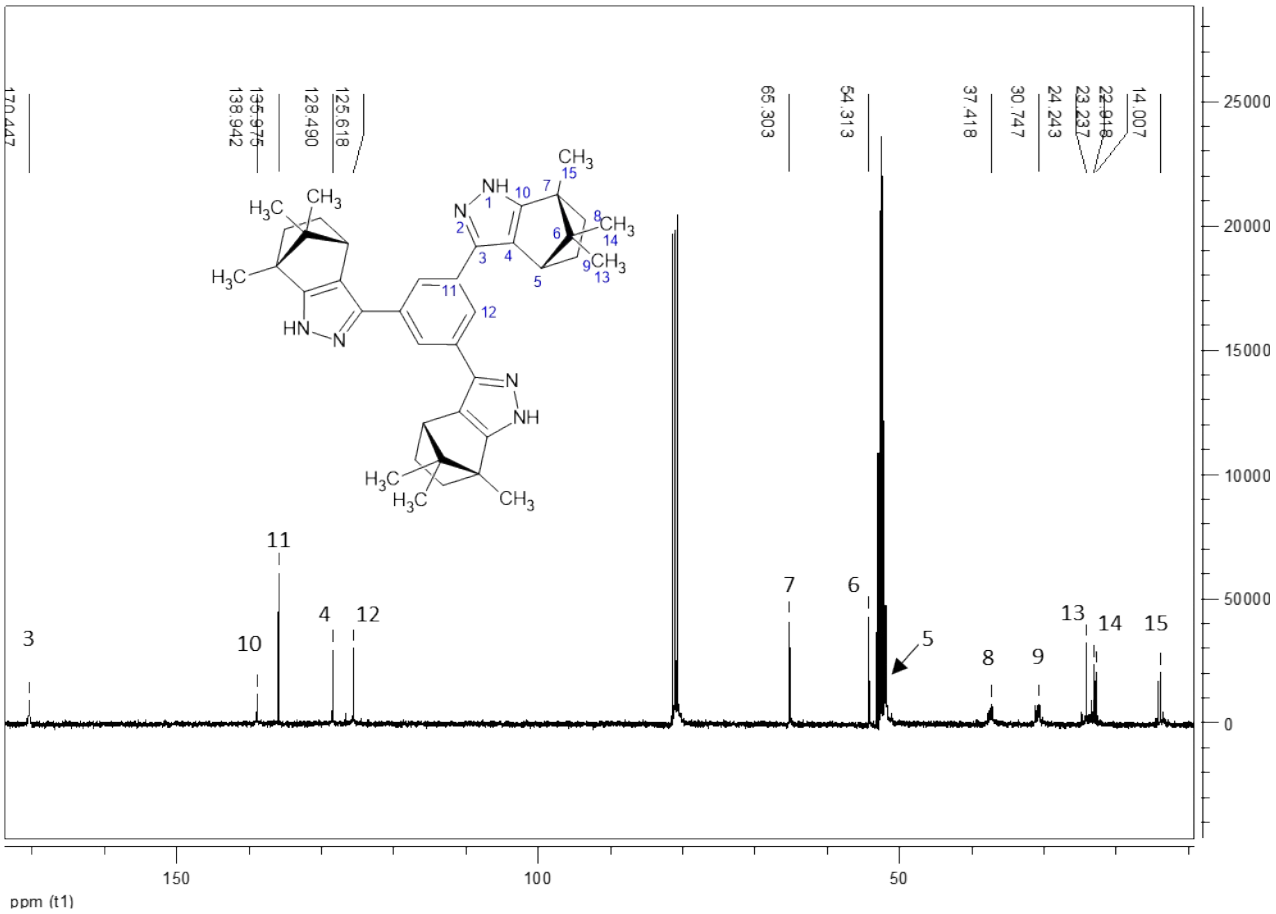


*Figure S 25:* $^{13}$C NMR of the **4S,7R-H$_3$tristmi** ligand (400 MHz, $CDCl_3$:MeOD = 5:1, 20°C).

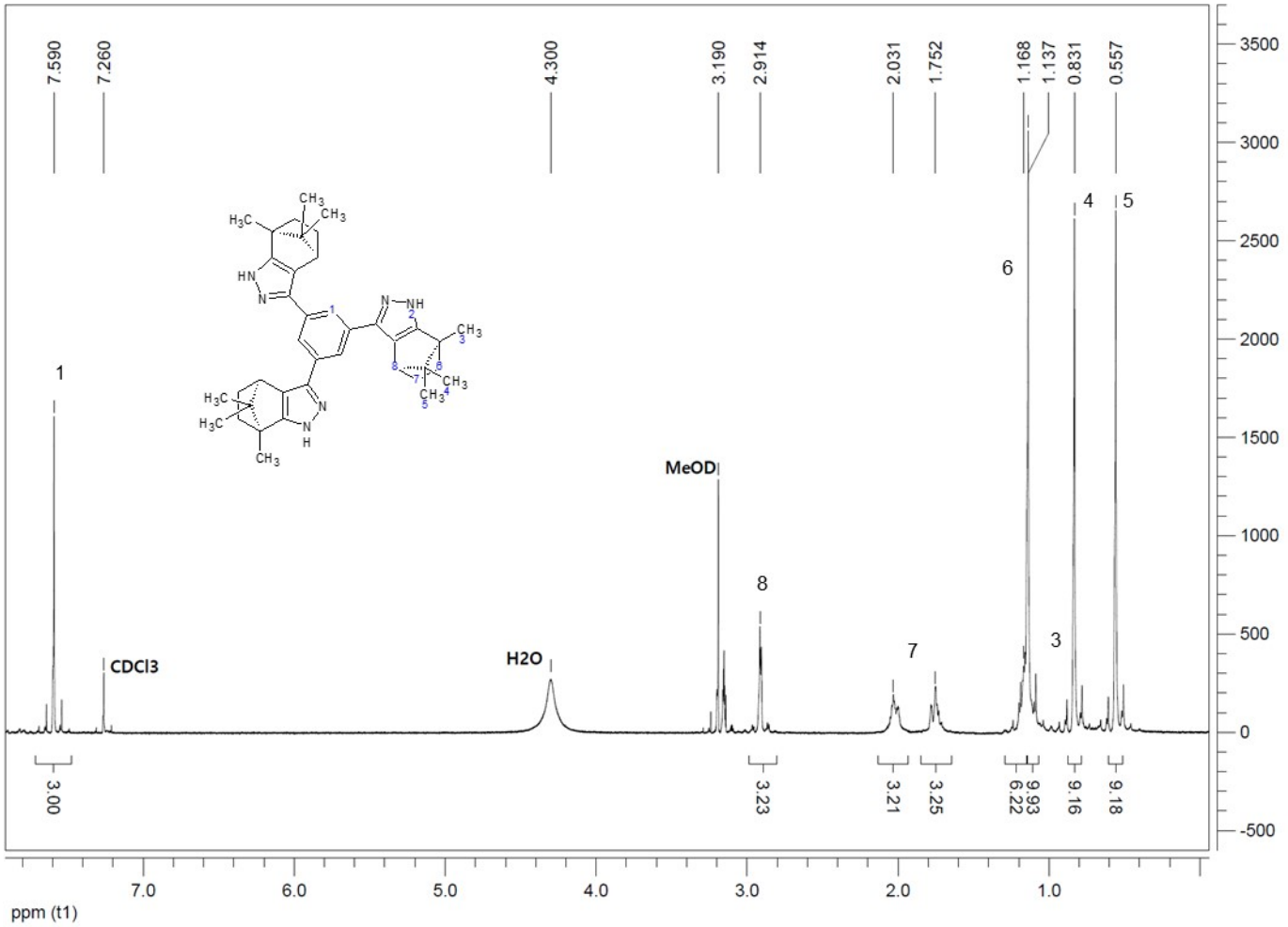


*Figure S 26:* $^{1}$H-NMR of the **4R,7S-H$_3$tristmi** ligand (400 MHz, $CDCl_3$:MeOD = 5:1, 20°C).

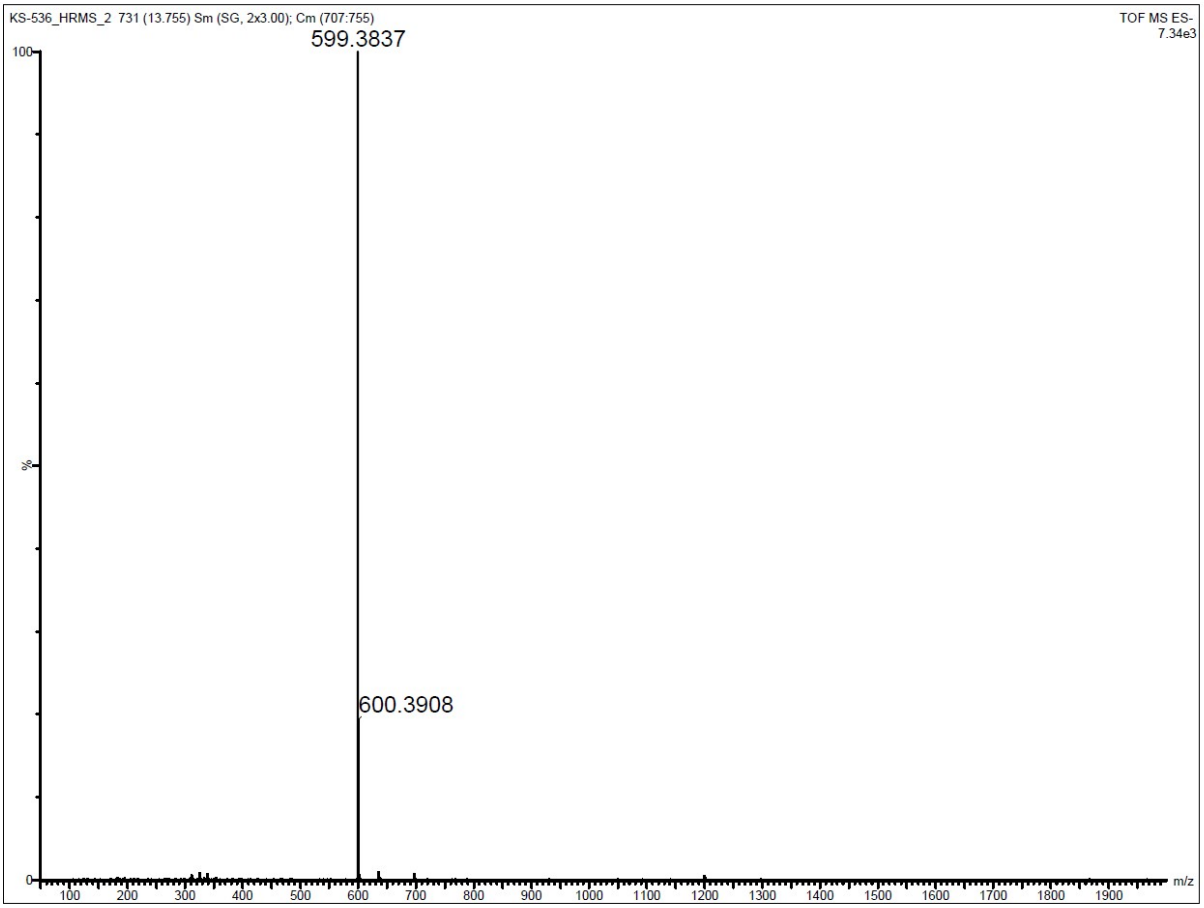


*Figure S 27:* HR-ESI(-)-MS of the **4S,7R-H$_3$tristmi** ligand; [$C_{39}H_{48}N_6$ - $H^-$]$^-$ requires 599.3868; found m/z 599.3837.

# 5. Microscopy

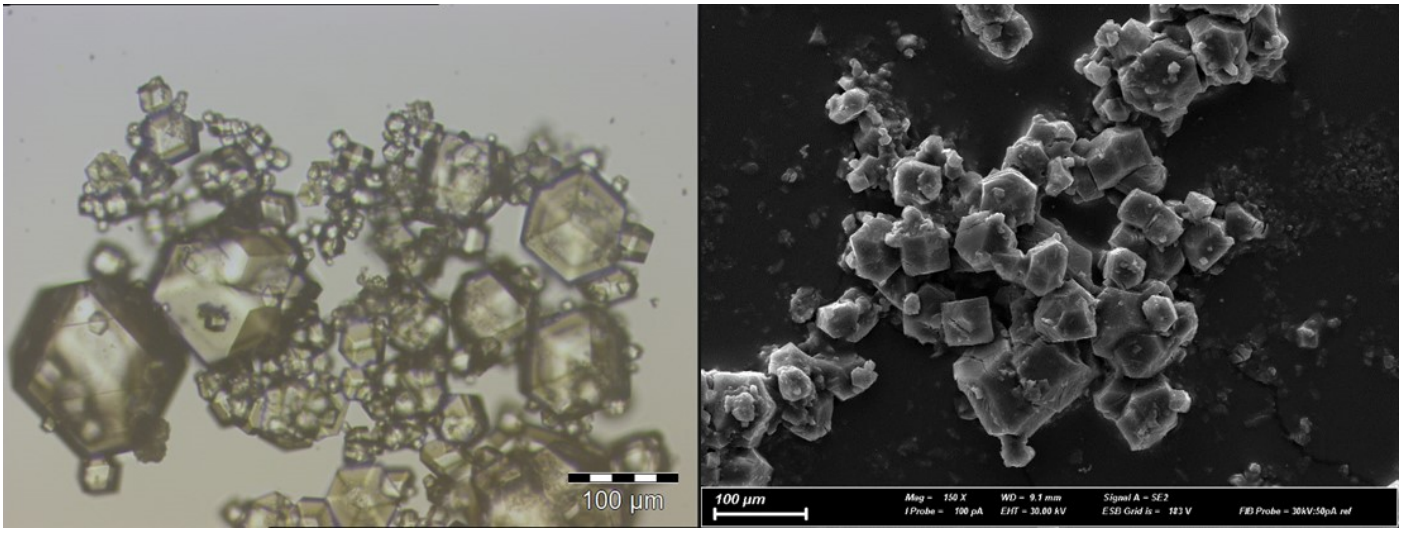


*Figure S 28:* Optical microscopy (left) and electron microscopy images of **IPA@4S,7R-CFA-22**.

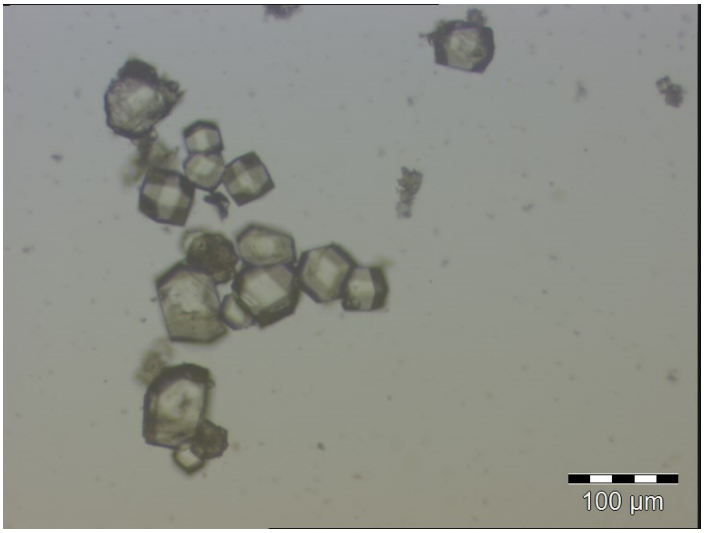


*Figure S 29:* Optical microscopy image of **IPA@4R,7S-CFA-22**.

# 6. PXRD Patterns

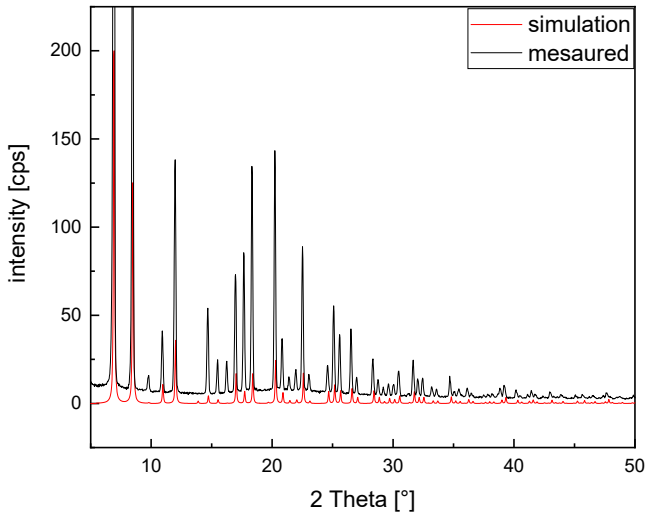


*Figure S 30:* PXRD-pattern of **IPA@4S,7R-CFA-22** (black) measured with the PANalytical (Empyran) diffractometer and PXRD-pattern simulated from single crystal measurement data (red).

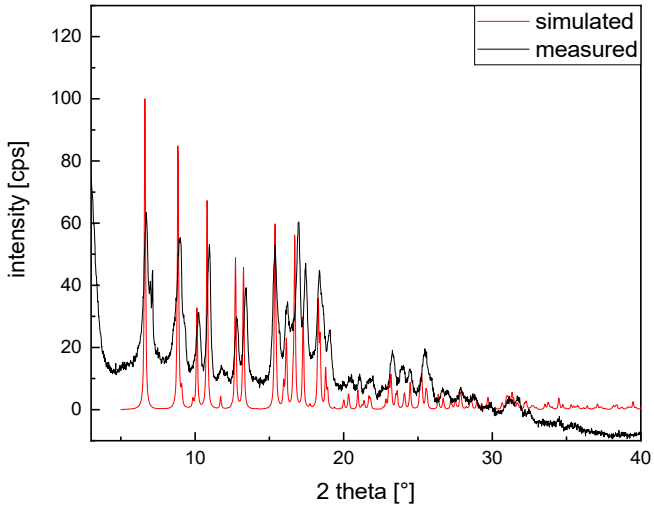


*Figure S 31:* Measured PXRD-pattern of **IPA@4R,7S-CFA-22** (black) and PXRD-pattern simulated from single crystal measurement data (red).

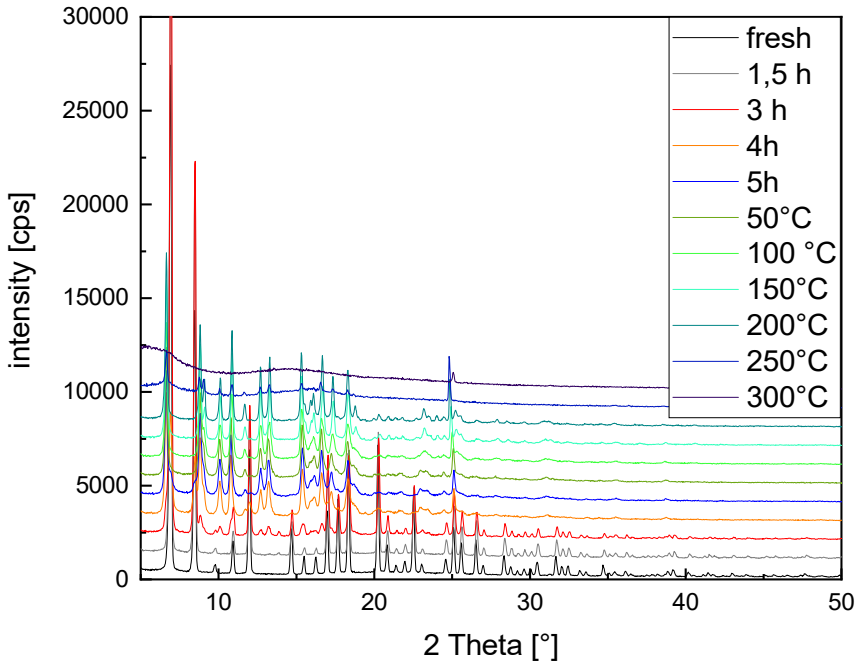


*Figure S 32:* VT-PXRD patterns of **IPA@4S,7R-CFA-22**.

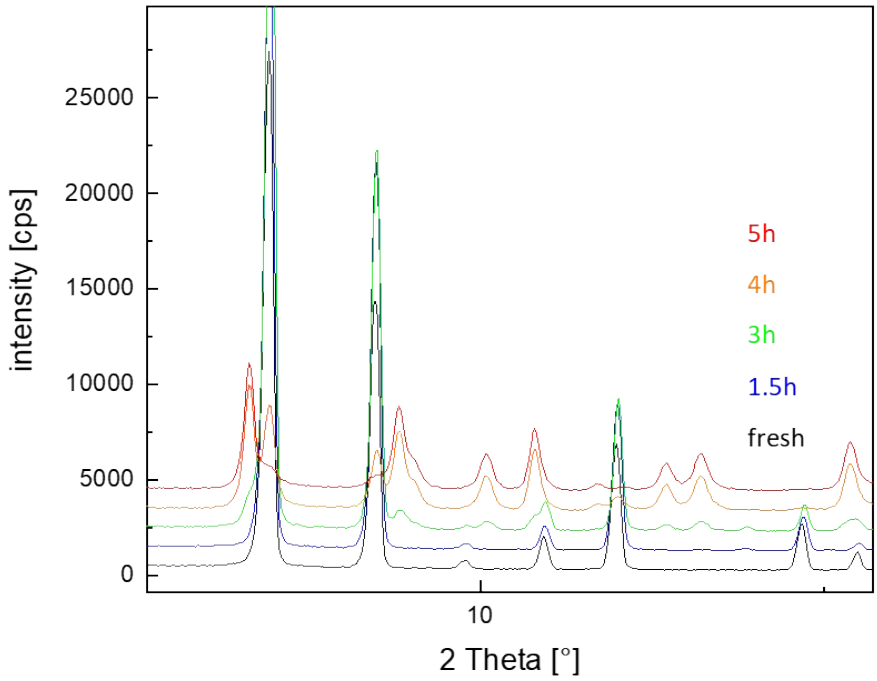


*Figure S 33:* Detailed view of the PXRD pattern changes upon drying of **IPA@4S,7R-CFA-22**.

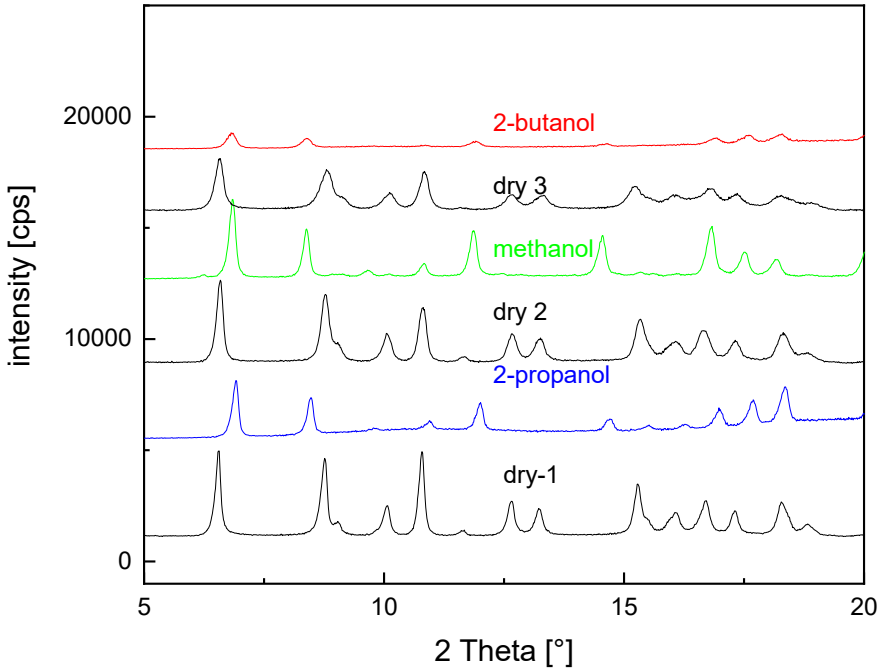


*Figure S 34:* Powder diffraction patterns of solvent exchange experiments. **4S,7R-CFA-22-dry** (black) and **solvent@4S,7R-CFA-22** (blue, green, red) can be converted into each other fully reproducible. Shown here with the same material dried three times (dry 1,2 and 3) after wetting with different solvents starting from the dry material.

# 7. TGA

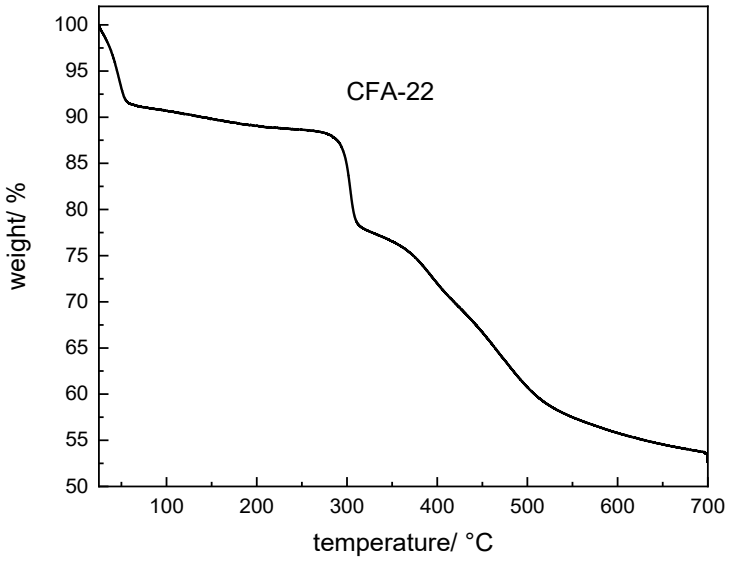


*Figure S 35:* TGA curve of ***4S,7R-CFA-22-dry***.

# 8. EDX

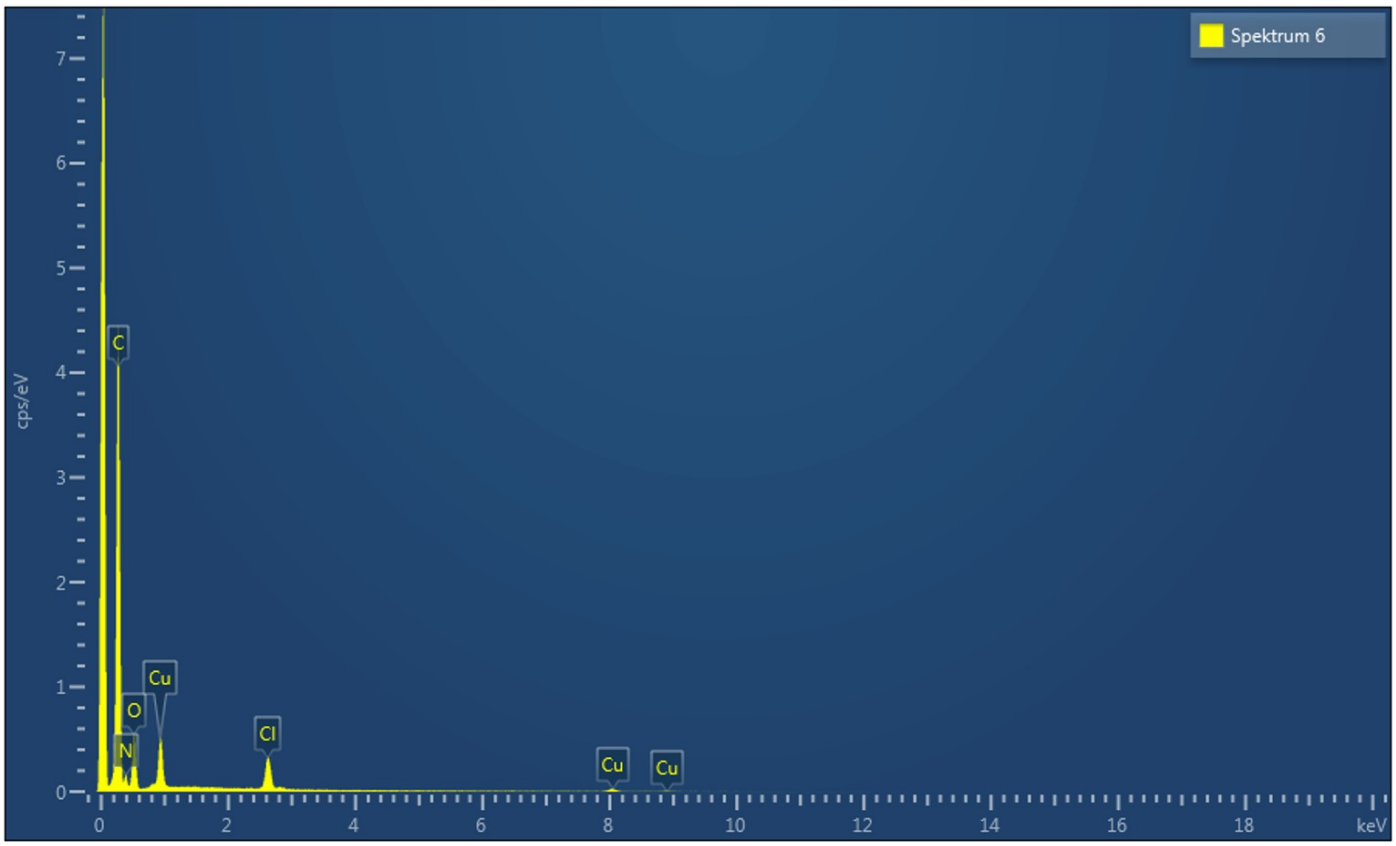


*Figure S 36:* EDX-Spectrum ***4S,7R-CFA-22-dry***.

Table S5: Results of EDX-measurement of **4S,7R-CFA-22-dry** averaged 6 spectra.

| Statistic | N | Cl | Cu |
|---|---|---|---|
| Max. | 57.73 | 29.84 | 30.64 |
| Min. | 39.52 | 18.90 | 22.90 |
| average | 50.34 | 23.82 | 25.85 |
| Standard deviation | 7.02 | 4.99 | 2.96 |

# 9. IR

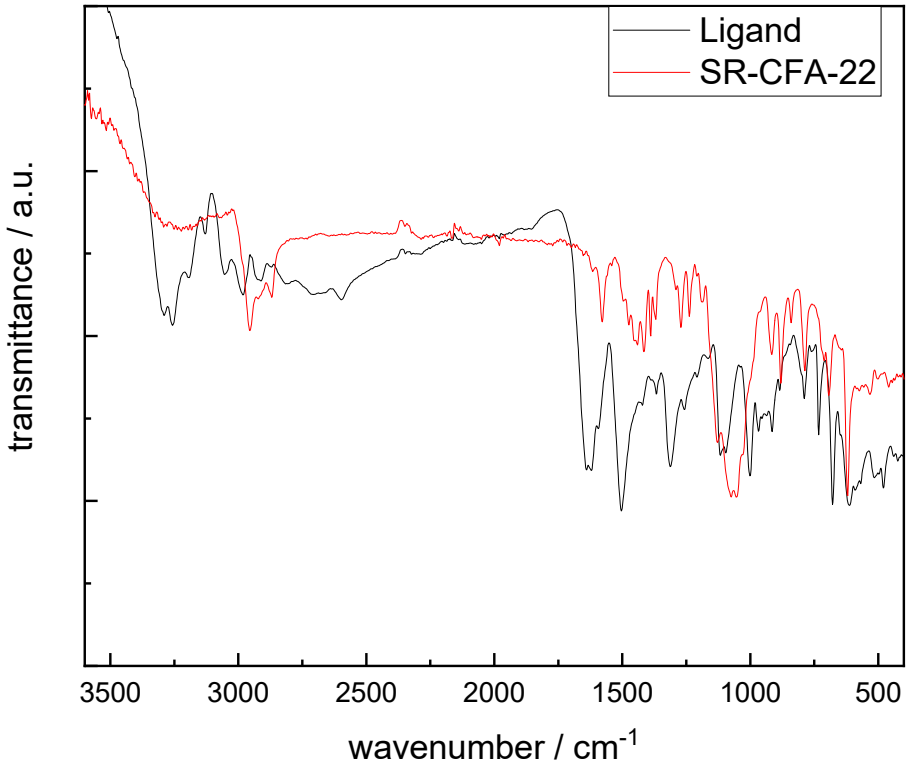


*Figure S 37:* Comparison of FT-IR spectra of the **4S,7R-H$_3$-tristmi** ligand (black) and **4S,7R-CFA-22-dry** (red).

# 10. References

(1) SAINT, Bruker Analytical X-Ray Systems Inc, Madison, WI, 2015.

(2) Krause, L.; Herbst-Irmer, R.; Sheldrick, G. M.; Stalke, D. Comparison of silver and molybdenum microfocus X-ray sources for single-crystal structure determination. *J. Appl. Cryst.* **2015**, *48* (Pt 1), 3–10. DOI: 10.1107/S1600576714022985. Published Online: Jan. 30, 2015.

(3) Sheldrick, G. M. SHELXT - integrated space-group and crystal-structure determination. *Acta Crystallogr., Sect. A: Found. Crystallogr.* **2015**, *71* (Pt 1), 3–8. DOI: 10.1107/S2053273314026370. Published Online: Jan. 1, 2015.

(4) Sheldrick, G. M. Crystal structure refinement with SHELXL. *Acta Crystallogr., Sect. C: Struct. Chem.* **2015**, *71* (Pt 1), 3–8. DOI: 10.1107/S2053229614024218. Published Online: Jan. 1, 2015.

(5) Spek, A. L. Structure validation in chemical crystallography. *Acta Cryst. D* **2009**, *65* (Pt 2), 148–155. DOI: 10.1107/S090744490804362X. Published Online: Jan. 20, 2009.

(6) Flack, H. D.; Bernardinelli, G. Absolute structure and absolute configuration. *Acta Cryst.* **1999**, *55* (Pt 5), 908–915. DOI: 10.1107/S0108767399004262.